A STRUCTURE AND ASYMPTOTIC PRESERVING SCHEME FOR THE QUASINEUTRAL LIMIT OF THE VLASOV-POISSON SYSTEM

Alain Blaustein[1], Giacomo Dimarco[2], Francis Filbet[3] and Marie-Hélène Vignal[4]

Abstract. In this work, we propose a new numerical method for the Vlasov–Poisson system that is both asymptotically consistent and stable in the quasineutral regime, *i.e.* when the Debye length is small compared to the characteristic spatial scale of the physical domain. Our approach consists in reformulating the Vlasov–Poisson system as a hyperbolic problem by applying a spectral expansion in the basis of Hermite functions in the velocity space and in designing a structure-preserving scheme for the time and spatial variables. Through this Hermite formulation, we establish a convergence result for the electric field toward its quasineutral limit together with optimal error estimates. Following the same path, we then propose a fully discrete numerical method for the Vlasov-Poisson system, inspired by the approach in [6], and rigorously prove that it is uniformly consistent in the quasineutral limit regime. Finally, we present several numerical simulations to illustrate the behavior of the proposed scheme. These results demonstrate the capability of our method to describe quasineutral plasmas and confirm the theoretical findings: conditional stability and asymptotic preservation.

Contents

2010 *Mathematics Subject Classification.* Primary: 82C40, 35Q83 Secondary: 65N08, 65N35 .
Key words and phrases. Vlasov-Poisson; quasineutral plasma; Hermite spectral method.

[1]alain.blaustein@inria.fr, Centre Inria de l'Université de Lille, France.
[2]giacomo.dimarco@unife.it, Università di Ferrara, Department of Mathematics and Computer Science & Center for Modeling, Computing and Statistics (CMCS), Ferrara, Italy.
[3]francis.filbet@math.univ-toulouse.fr, Institut de Mathématiques de Toulouse, Université de Toulouse, France.
[4]mhvignal@math.univ-toulouse.fr, Institut de Mathématiques de Toulouse, Université de Toulouse, France.

1. Introduction

Plasma flows are multiscale problems, involving interactions that span from microscopic to macroscopic scales [12]. As a result, the numerical simulation of plasmas presents a significant challenge for both the computational physics and applied mathematics communities. Depending on the physical regime of interest, plasmas are typically described by two main classes of mathematical models: fluid [15] or kinetic [23]. Fluid models describe the evolution of macroscopic quantities, such as density, temperature, and mean velocity and remain valid when the plasma is close to thermodynamical equilibrium. In contrast, kinetic models consider the time evolution of a distribution function in six-dimensional phase space, representing the probability of a particle occupying a given state at any moment. While these models are able to describe a broader range of physical regimes, they are significantly more computationally demanding.

In this paper, we focus on plasmas far from equilibrium and therefore we adopt a kinetic perspective based on the Vlasov–Poisson system. Specifically, we investigate the role of quasineutrality and the challenges it presents. Quasineutrality refers to the assumption that, on macroscopic scales, the net charge density in the plasma is effectively zero. Under this assumption, it is not possible to solve the electric field generated by local charge separations. Instead, the macroscale behavior of the system can be captured referring to asymptotic models, where the electric field is determined through constraints on the density and velocity divergence. However, in certain scenarios, quasineutrality and charge imbalances may coexist. This makes challenging the development of numerical methods capable of accurately capturing both effects. Addressing this issue remains an active area of investigation [1, 3, 13, 14, 17, 18, 19] and the work here proposed goes in the direction of contributing to this research.

In particular, in this work, we combine a theoretical analysis of the behavior of the Vlasov-Poisson system in the quasineutral regime with the design of a new numerical method capable of resolving the challenges related to its description. The physical model studied involves several interacting scales, among which the Debye length λ_D and the electron plasma period ω_p^{-1} play a fundamental role:

$$\lambda_D := \sqrt{\frac{\varepsilon_0\, k_B\, T_0}{n_0\, e^2}}, \qquad \omega_p^{-1} := \sqrt{\frac{n_0\, e^2}{\varepsilon_0\, m}}, \tag{1.1}$$

where n_0 and T_0 are the characteristic density and temperature, e is the elementary charge, ε_0 the vacuum permittivity, k_B the Boltzmann constant, and m the electron mass. The Debye length defines the characteristic scale at which charge imbalances occur, while the electron plasma period represents the characteristic oscillation time associated with electrostatic forces that restore electric neutrality when charge imbalances arise at the Debye length scale [16]. When both the Debye length and the plasma period are small compared to the macroscopic scales of interest, the quasineutral regime holds true and the plasma appears broadly electrically neutral. In the sequel we introduce the details of the model employed.

1.1. The mathematical model and review.

Let us first introduce the mathematical model and analyze the different scales involved. The Vlasov-Poisson system provides a kinetic description of a gas constituted of charged particles interacting through a electric field:

$$\begin{cases} \dfrac{\partial f}{\partial t} + v\cdot\nabla_x f + \dfrac{q}{m}E\cdot\nabla_v f = 0\,, \\[2ex] E = -\nabla_x\phi \ ; \ -\varepsilon_0\Delta_x\phi = q\,(\rho-\rho_i) \ ; \ \rho = \displaystyle\int_{\mathbb{R}^3} f\,\mathrm{d}v\,. \end{cases} \tag{1.2}$$

In (1.2), $f(t,x,v)$ is the distribution of electrons over the phase space $(x,v)\in\mathbb{T}^3\times\mathbb{R}^3$ at time $t\geq 0$. Interactions are taken into account thanks to a coupling between kinetic and Poisson equations (first and second line of (1.2) respectively). The constant q expresses the elementary charge $q=-e<0$, the scalar function ϕ is the electric potential, while the macroscopic densities of electrons and ions are denoted respectively by $\rho(t,x)$ and $\rho_i(t,x)=\rho_i(x)$. Let us note that in system (1.2), one supposes the ions to represent a prescribed fixed background. This assumption while on one side simplifies the dynamics, on the other side it allows to focus on the fundamental aspects of the quasineutrality mechanism avoiding unessential features.

We introduce now the rescaled parameter λ given by

$$\lambda = \frac{\lambda_D}{L} = \left(\frac{\varepsilon_0\, k_B T_0}{L^2 e^2\, n_0}\right)^{1/2},$$

where L represents the characteristic length at which the physical phenomena are studied, in our case it corresponds to the length of the electric field interactions in plasmas. The quasineutral regime corresponds instead to the limit of the Vlasov-Poisson system when $\lambda \to 0$. This asymptotic limit has been extensively studied in the past by several authors from both the numerical and theoretical points of view. For a theoretical analysis in the context of kinetic and fluid models, see for example [10, 27, 25, 28, 8, 7] and the references therein. The study of the quasineutral limit is often based on reformulation of the Vlasov-Poisson system with respect to the adimensional parameter λ and then in passing to the limit λ going to zero in this rescaled system. Here, we restrict ourselves to the rescaled one dimensional in space and in velocity setting. This leads to the following equations, see in [14, 16] for details,

$$
\left\{
\begin{aligned}
&\partial_t f^\lambda + v\,\partial_x f^\lambda + E^\lambda\,\partial_v f^\lambda = 0\,,\\
&E^\lambda = -\partial_x\phi^\lambda\,;\; -\lambda^2\partial_x^2\phi^\lambda = \rho^\lambda - 1\,;\; \rho^\lambda(t,x) = \int_{\mathbb{R}} f^\lambda(t,x,v)\,\mathrm{d}v\,,
\end{aligned}
\right.
\tag{1.3}
$$

where $f^\lambda(t,x,v)$, is the distribution at time $t \geq 0$ over the phase-space $(x,v) \in \mathbb{T}\times\mathbb{R}$ and where the density of the ions is assumed to be constant and equal to one everywhere in space. The following condition ensures the uniqueness of ϕ^λ

$$
\int_{\mathbb{T}} \phi^\lambda(t,x)\,\mathrm{d}x = 0\,.
\tag{1.4}
$$

The model (1.3)-(1.4) possesses the following key properties: conservation of total charge, of total flux (set to 0 for simplicity and without loss of generality) and conservation of the global energy. These read

$$
\left\{
\begin{aligned}
&\int_{\mathbb{T}} \rho^\lambda(t,x)\,\mathrm{d}x = \int_{\mathbb{T}} \rho^\lambda(0,x)\,\mathrm{d}x = |\mathbb{T}|\,,\\
&\int_{\mathbb{T}} j^\lambda(t,x)\,\mathrm{d}x = \int_{\mathbb{T}} j^\lambda(0,x)\,\mathrm{d}x = 0\,,\\
&\int_{\mathbb{T}} K^\lambda(t,x) + \lambda^2\left|E^\lambda(t,x)\right|^2\mathrm{d}x = \int_{\mathbb{T}} K^\lambda(0,x) + \lambda^2\left|E^\lambda(0,x)\right|^2\mathrm{d}x\,,
\end{aligned}
\right.
\tag{1.5}
$$

where the flux j^λ (also called the current density in the rest of the paper) and the kinetic energy K^λ are given by

$$
\left\{
\begin{aligned}
&j^\lambda(t,x) = \int_{\mathbb{R}} v f^\lambda(t,x,v)\,\mathrm{d}v\,,\\
&K^\lambda(t,x) = \int_{\mathbb{R}} |v|^2 f^\lambda(t,x,v)\,\mathrm{d}v\,.
\end{aligned}
\right.
\tag{1.6}
$$

From a numerical perspective, traditional explicit schemes applied to (1.3) must resolve the microscopic scales related to the small parameter λ^2 to ensure stability and consistency with the limit $\lambda \to 0$. However, this requirement necessitates extremely small time steps and phase space discretizations in order to remain stable. At the same time, numerical simulations consider macroscopic scales in order to catch significant phenomena. This situations creates important computational challenges and it causes these methods impractical for realistic applications. While asymptotic models can be derived to describe macroscopic regimes, again additional challenges arise in scenarios where quasineutral and non-quasineutral regions coexist making simulations particularly difficult.

To address this complexity, domain decomposition approaches or hybrid methods can be employed [11, 20, 22, 24]. However, integrating different models and numerical methods requires care, and accurately identifying interfaces remains a challenging task which has not been yet fully accomplished. Therefore, it is crucial to design numerical methods capable of handling multiple regimes simultaneously, without being constrained by small-scale dynamics. The development of schemes that work without such limitations has been the focus of extensive research in the recent years. This is precisely the area in which Asymptotic Preserving (AP) methods have been created, see [29, 21] and [30] for a recent review on the subject. These methods can bypass the above discussed restrictions while automatically achieving transition to consistent discretizations of limiting models as the parameters characterizing microscopic behavior approach zero. The use of Asymptotic Preserving in the context of quasineutrality has been investigated for instance in [14] by some of the authors of the present work. They proposed a first-order-in-time scheme and a linear stability analysis proving indeed stability for small values of the Debye length of the proposed method. The concept revolved about the reformulation and the consequent discretization of the Poisson equation. This idea was initially introduced in [13] and later used in [3] and [1, 18, 19, 17] in subsequent researches. For a general review of numerical methods capturing the quasineutral limit for both kinetic and fluid models, we refer to [16]. In this work, we adopt an alternative approach. This mainly consists of two parts. In the first part, we study relevant analytical properties of the Vlasov–Poisson system close to the quasineutral limit. In the second part, based on the theoretical results obtained, we introduce a new numerical method and, for this scheme, we perform a discrete counterpart analysis. This, in particular, permits to highlight the main properties of the proposed scheme such as conditional stability and preservation of the asymptotic state. Unlike previous approaches in the literature [13, 14, 16], our discretization does not rely on reformulating the Poisson equation as an equivalent harmonic oscillator equation. Instead, we discretize the Poisson equation concurrently with the equations governing the time evolution of the first moments of the distribution function. Finally, we stress that, part of our numerical investigations discussed in the last part of this work, consists in focusing on scenarios where the results of theoretical analysis does not hold true anymore. In particular, by studying these cases, we aim to identify the necessary precautions to avoid physically irrelevant results.

In the following section, we first recall the formal limit of the Vlasov–Poisson system as the Debye length approaches zero (Section 1.2). Then, in Section 2, we reformulate the Vlasov–Poisson system as a hyperbolic system with source terms by expanding the distribution function in velocity using a basis of Hermite functions. This reformulation is particularly well-suited for studying the quasineutral limit, as we will demonstrate. Next, we establish a convergence result for the electric field toward its quasineutral limit by explicitly characterizing the oscillatory component of the solution (see Proposition 2.1) and highlighting the impact of the initial conditions on the size of these oscillations. Starting from this formulation, we propose a numerical scheme based on a time-splitting strategy in Section 3. We rigorously prove that the scheme captures the asymptotic behavior of the solution in Section 3.3. In Section 4, we present several numerical simulations to illustrate the behavior of the proposed discretization in relation to the theoretical results of Proposition 2.1, including an analysis of the error estimates. A last section 5 is dedicated to draw some conclusions and discuss some future developments.

1.2. **Formal quasineutral limit.** Let us now observe that in the regime $\lambda \ll 1$, the second line in (1.3) forces the global neutrality condition expressed by the first line of (1.5) to become a pointwise constraint in x. Indeed, one expects the solution f^λ to formally converge to the solution f of the quasineutral system

$$\left\{ \begin{aligned} & \partial_t f \,+\, v\,\partial_x f \,+\, E\,\partial_v f \,=\, 0\,, \\ & \rho(t,x) \,=\, 1\,;\ \rho(t,x) \,=\, \int_{\mathbb{R}} f(t,x,v)\,\mathrm{d}v\,, \end{aligned} \right. \tag{1.7}$$

where $f(t,x,v)$ is the limiting distribution over the phase-space $(x,v) \in \mathbb{T} \times \mathbb{R}$. The latter system may be confusing at first look, as the equation on the limiting field E seems to be missing. In fact, E remains fully determined even in (1.7), as it may be interpreted as the Lagrange multiplier associated to the pointwise neutrality constraint from the second line of equations (1.7). Indeed, the quasineutral limit described by system (1.7) together with the conditions (1.5) imposes the limiting electric field and the limiting electric flux to satisfy the following relations

$$\left\{ \begin{aligned} & j(t,x) \,=\, 0\,, \\ & E(t,x) \,=\, \partial_x K(t,x)\,, \end{aligned} \right. \tag{1.8}$$

where the kinetic energy K is given by (1.6). Hence, global conservation of the total charge and the total flux in (1.5) both become pointwise constraints in the quasineutral regime, according to the second line of (1.7) and the first line of (1.8) respectively.

Remark 1.1. *Let us observe that* (1.8) *is obtained multiplying the Vlasov equation* (1.7) *by* $(1, v)^t$ *and integrating over* $v \in \mathbb{R}$*. We then use the pointwise neutrality constraint and total conservation of flux for* $j(t,x)$*, and both pointwise neutrality and conservation of flux for obtaining the expression of the electric field* $E(t,x)$*.*

Before continuing, we point out that the quasineutral system may not be well-posed for all initial data. This was observed in [2] for the related Vlasov-Dirac-Benney system and in [28] near the so-called Penrose unstable profiles for the Vlasov-Poisson system. Indeed, in such cases, small perturbations from the quasineutral state can lead to the development of instabilities in the plasma. In order to try to shed light on this problem, in what follows, we investigate the solutions of the Vlasov-Poisson system near quasineutrality by restricting our analysis to configurations near Penrose stable profiles. However, in the numerical section, we will simulate both stable and unstable cases to illustrate different phenomena.

One of the key challenges in the numerical analysis and simulation of the quasineutral regime is that the strong convergence of f^λ to f may fail due to the emergence of fast oscillations with period $1/\lambda$ when $\lambda \ll 1$ in the solution, see for instance [27, 28, 8]. The intuition behind these oscillations is that the pointwise neutrality and conservation of flux in (1.7)-(1.8) may not be verified by the non neutral initial distribution $f^\lambda(t=0)$ giving rise to these phenomena. To uncover these oscillations, in the sequel, we determine their amplitude thanks to formal energy considerations. In particular, we focus on initial configurations with uniformly bounded total energy as $\lambda \ll 1$, that is

$$\sup_{\lambda>0}\left(\int_{\mathbb{T}} K^\lambda(0,x) + \lambda^2\left|E^\lambda(0,x)\right|^2 \mathrm{d}x\right) \,<\, +\infty\,.$$

Since total energy is conserved by (1.4), this yields for all $t \geq 0$

$$\sup_{\lambda>0}\left(\int_{\mathbb{T}} K^\lambda(t,x) + \lambda^2\left|E^\lambda(t,x)\right|^2 \mathrm{d}x\right) \,<\, +\infty\,.$$

In particular, this estimate indicates that E^λ is at most of order $O(\lambda^{-1})$

$$\sup_{\lambda>0}\left(\lambda\left\|E^\lambda(t)\right\|_{L^2(\mathbb{T})}\right) \,<\, +\infty\,; \quad \text{that is} \quad \left|E^\lambda(t)\right| \lesssim \frac{1}{\lambda}\,, \quad \text{as} \quad \lambda \ll 1\,,$$

which means that the amplitude of the electric field oscillations is at most of order $O\left(\lambda^{-1}\right)$. In the following, we restrict our investigation to cases characterized by smaller amplitudes of the electric field, namely

$$\left|E^\lambda(t)\right| \lesssim \frac{1}{\lambda^\alpha}\,, \quad \text{for some} \quad 0 \,\leq\, \alpha \,<\, 1\,, \quad \text{as} \quad \lambda \ll 1. \tag{1.9}$$

It is worth mentioning that the analysis of the critical case $\alpha = 1$ significantly differs from the cases where $\alpha < 1$ [27, 28]. We will discuss this critical case only in the section devoted to numerical simulations. Now, to identify the period of oscillations, we analyze the coupled system current density j^λ and electric field E^λ, which reads

$$\begin{cases} \lambda^2 \partial_t E^\lambda \,+\, j^\lambda \,=\, 0\,, \\[2ex] \partial_t\, j^\lambda \,+\, \partial_x K^\lambda \,-\, \rho^\lambda\, E^\lambda \,=\, 0\,. \end{cases} \tag{1.10}$$

This is obtained multiplying the Vlasov equation in (1.3) by $(1,v)^t$, integrating over $v \in \mathbb{R}$ and then substituting the Poisson equation in the continuity equation. We now rewrite the coupled system (1.10) as

$$\partial_t \begin{pmatrix} E^\lambda - \partial_x K^\lambda \\[1ex] \lambda^{-1}\, j^\lambda \end{pmatrix} \,+\, \frac{1}{\lambda}\, J \cdot \begin{pmatrix} E^\lambda - \partial_x K^\lambda \\[1ex] \lambda^{-1}\, j^\lambda \end{pmatrix} \,+\, \mathbf{R}^\lambda \,=\, 0\,, \tag{1.11}$$

where the matrix J and the vector $\mathbf{R}^\lambda$ are given as follows

$$J \,=\, \begin{pmatrix} 0 & 1 \\[1ex] -1 & 0 \end{pmatrix}\,, \quad \text{and} \quad \mathbf{R}^\lambda \,=\, \begin{pmatrix} \partial_{tx} K^\lambda \\[2ex] \lambda^{-1}\,\left(1-\rho^\lambda\right) E^\lambda \end{pmatrix}\,.$$

Equation (1.11) shows that the electric field and the flux behave like harmonic oscillators with period $1/\lambda$ up to the source term $\mathbf{R}^\lambda$. Indeed, multiplying (1.11) by the matrix $\exp\left(tJ/\lambda\right)$ and integrating in time, we obtain the following Duhamel formula

$$\begin{pmatrix} E^\lambda - \partial_x K^\lambda \\[1ex] \lambda^{-1}\, j^\lambda \end{pmatrix}(t) \,=\, \exp\left(-\frac{t}{\lambda}\, J\right) \cdot \begin{pmatrix} E^\lambda - \partial_x K^\lambda \\[1ex] \lambda^{-1}\, j^\lambda \end{pmatrix}(0) \,-\, \int_0^t \exp\left(\frac{s-t}{\lambda}\, J\right) \cdot \mathbf{R}^\lambda(s)\,\mathrm{d}s\,,$$

for all time $t \geq 0$, where $\exp\left(tJ\right)$ is the rotation matrix with angle t:

$$\exp\left(tJ\right) \,=\, \begin{pmatrix} \cos\left(t\right) & \sin\left(t\right) \\[1ex] -\sin\left(t\right) & \cos\left(t\right) \end{pmatrix}\,. \tag{1.12}$$

The difficulty is then to prove that, under the conditions (1.9), the remainder in the Duhamel formula may be neglected in the regime $\lambda \ll 1$ (see also [27, 28, 8]), which yields

$$
(1.13) \qquad \left\{
\begin{aligned}
E^\lambda(t) &\underset{\lambda \ll 1}{\simeq} \partial_x K^\lambda(t) + \cos\left(\frac{t}{\lambda}\right)\left(E^\lambda - \partial_x K^\lambda\right)(0) - \frac{1}{\lambda}\sin\left(\frac{t}{\lambda}\right) j^\lambda(0)\,,\\
j^\lambda(t) &\underset{\lambda \ll 1}{\simeq} 0 + \lambda \sin\left(\frac{t}{\lambda}\right)\left(E^\lambda - \partial_x K^\lambda\right)(0) + \cos\left(\frac{t}{\lambda}\right) j^\lambda(0)\,.
\end{aligned}
\right.
$$

These formal computations show that the quasi neutral limit (1.8) is satisfied up to fast oscillations of period $1/\lambda$ with amplitude only depending on the initial data $f^\lambda(t=0)$.

We will in the sequel make the above analysis rigorous thanks to the Hermite framework.

2. Hermite formulation of the quasineutral regime

The Hermite decomposition arises naturally when studying the Vlasov-Poisson system. It corresponds to a moment method tailored with an additional spectral structure and well suited for accurate numerical approximations. We start by recasting (1.3) and (1.7) in the Hermite framework, successively we highlight how quasineutral oscillations naturally uncover in this setting.

2.1. The Hermite framework.

We decompose the distribution f^λ and its quasineutral counterpart f into their Hermite components (coefficients) $C^\lambda = \left(C_k^\lambda\right)_{k\in\mathbb{N}}$ and $C = (C_k)_{k\in\mathbb{N}}$, that is,

$$
(2.1) \qquad f^\lambda(t,x,v) = \sum_{k\in\mathbb{N}} C_k^\lambda(t,x)\, \Psi_k(v) \quad \text{and} \quad f(t,x,v) = \sum_{k\in\mathbb{N}} C_k(t,x)\, \Psi_k(v)\,,
$$

where the basis of Hermite functions $(\Psi_k)_{k\in\mathbb{N}}$ is defined recursively as follows $\Psi_{-1} = 0$, $\Psi_0 = \mathcal{M}$ and

$$
(2.2) \qquad v\,\Psi_k(v) = \sqrt{T_0 k}\,\Psi_{k-1}(v) + \sqrt{T_0(k+1)}\,\Psi_{k+1}(v)\,, \quad \forall\, k \geq 0\,,
$$

and where $\mathcal{M}$ denotes the stationary Maxwellian with fixed temperature $T_0 > 0$

$$
(2.3) \qquad \mathcal{M}(v) = \frac{1}{\sqrt{2\pi\, T_0}} \exp\left(-\frac{|v|^2}{2\,T_0}\right).
$$

Hermite functions $(\Psi_k)_{k\in\mathbb{N}}$ constitute an orthonormal system for the inverse Gaussian weight:

$$
(2.4) \qquad \int_{\mathbb{R}} \Psi_k(v)\,\Psi_l(v)\,\mathcal{M}^{-1}(v)\mathrm{d}v = \delta_{k,l}\,,
$$

where $\delta_{k,l}$ denotes the Kronecker symbol ($\delta_{k,l} = 1$ when $k = l$ and $\delta_{k,l} = 0$ otherwise). The decomposition (2.1) may also be interpreted as a moment method, where C_k, $k \geq 0$, stands for the moment of the distribution of order k, appropriately modified in order to satisfy the orthogonality constraint (2.4). In particular, from (2.1) one can easily retrieve the macroscopic quantities associated to f^λ. For example, mass (1.3), current density and kinetic energy (1.6) are given by

$$
\rho^\lambda(t,x) = C_0^\lambda(t,x)\,; \quad j^\lambda(t,x) = \sqrt{T_0}\,C_1^\lambda(t,x)\,; \quad K^\lambda(t,x) = T_0\left(\sqrt{2}\,C_2^\lambda + C_0^\lambda\right)(t,x)\,.
$$

Thanks to the above decomposition, one can rewrite (1.3) and (1.7) as infinite hyperbolic systems with unknowns $C^\lambda = \left(C_k^\lambda\right)_{k\in\mathbb{N}}$ and $C = (C_k)_{k\in\mathbb{N}}$, where the discrete spectral parameter $k \in \mathbb{N}$ now replaces the velocity variable $v \in \mathbb{R}$. More precisely, for each $k \geq 0$, we compute the equation for C_k^λ by multiplying (1.3) with $\Psi_k\,\mathcal{M}^{-1}$ and integrating over $v \in \mathbb{R}$. We then use (2.2) to compute the contribution of the free transport operator $v\,\partial_x$ and the following relation to compute the field contribution $\partial_x\phi^\lambda\partial_v$

$$
\partial_v\left(\Psi_k\,\mathcal{M}^{-1}\right) = \sqrt{\frac{k}{T_0}}\,\Psi_{k-1}\,\mathcal{M}^{-1}\,, \quad \forall\, k \geq 0\,.
$$

Finally, the orthogonality property (2.4) is used to close the systems of equations. This yields for the coefficients $C^\lambda = (C_k^\lambda)_{k\in\mathbb{N}}$ the following coupled system

$$
(2.5) \qquad \left\{
\begin{aligned}
&\partial_t C_k^\lambda + \sqrt{T_0\,k}\,\partial_x C_{k-1}^\lambda + \sqrt{T_0\,(k+1)}\,\partial_x C_{k+1}^\lambda - \sqrt{\frac{k}{T_0}}\,E^\lambda\,C_{k-1}^\lambda = 0\,, \qquad \forall\, k \in \mathbb{N}\,,\\
&E^\lambda = -\partial_x\phi^\lambda\,;\ -\lambda^2\partial_x^2\phi^\lambda = C_0^\lambda - 1\,,
\end{aligned}
\right.
$$

where we have set $C^\lambda_{-1} = 0$, whereas the Hermite coefficients $C = (C_k)_{k\in\mathbb{N}}$ related to the asymptotic distribution $f(t,x,v)$ satisfy

$$
(2.6)\qquad \begin{cases} C_0 \,=\, 1\,, \\ C_1 \,=\, 0\,, \\ \partial_t C_k \,+\, \sqrt{T_0\,k}\,\partial_x C_{k-1} \,+\, \sqrt{T_0\,(k+1)}\,\partial_x C_{k+1} \,-\, \sqrt{\dfrac{k}{T_0}}\,E\,C_{k-1} \,=\, 0\,, \qquad \forall\, k\geq 2\,, \\ E \,=\, \sqrt{2}\,T_0\,\partial_x C_2\,. \end{cases}
$$

In the next section, using the Hermite framework introduced above, we justify the formal computations presented in Section 1.2.

2.2. **Continuous analysis of the quasineutral regime.** To compute the oscillatory components of (f^λ,ϕ^λ) within the Hermite framework, we first rewrite the Ampère and flux equations (1.10) as

$$
(2.7)\qquad \lambda^2\partial_t E^\lambda \,+\, \sqrt{T_0}\,C_1^\lambda \,=\, 0\,, \quad \text{and} \quad \partial_t C_1^\lambda \,+\, \sqrt{T_0}\,\partial_x C_0^\lambda \,+\, \sqrt{2\,T_0}\,\partial_x C_2^\lambda \,-\, \frac{1}{\sqrt{T_0}}\,E^\lambda\,C_0^\lambda \,=\, 0\,.
$$

Therefore, the system (1.11) takes the form

$$
(2.8)\qquad \partial_t \begin{pmatrix} E^\lambda - E^\lambda_{\text{slow}} \\ \lambda^{-1}\sqrt{T_0}\,C_1^\lambda \end{pmatrix} \,+\, \frac{1}{\lambda}\,J\cdot \begin{pmatrix} E^\lambda - E^\lambda_{\text{slow}} \\ \lambda^{-1}\sqrt{T_0}\,C_1^\lambda \end{pmatrix} \,+\, \mathbf{S}^\lambda \,=\, 0\,,
$$

where J is defined in (1.11) and $\mathbf{S}^\lambda$ is given by

$$
\mathbf{S}^\lambda \,=\, \begin{pmatrix} \sqrt{2}\,T_0\,\partial_t\partial_x C_2^\lambda \\ \lambda^{-1}(T_0\,\partial_x C_0^\lambda \,+\, E^\lambda\,(1-C_0^\lambda)) \end{pmatrix}.
$$

The quantity E^λ_{slow} plays the role of the quasineutral electric field and it is defined by

$$
E^\lambda_{\text{slow}} := \sqrt{2}\,T_0\partial_x C_2^\lambda\,.
$$

In the introduction, we interpreted system (2.8) as a coupled harmonic oscillator up to a source term $\mathbf{S}^\lambda$. To justify this statement, we now analyze the behavior of $E^\lambda - E^\lambda_{\text{slow}}$ and C_1^λ in time. To this aim, we define $\mathbf{U}^\lambda$ as

$$
\mathbf{U}^\lambda(t) \,:=\, \begin{pmatrix} E^\lambda - E^\lambda_{\text{slow}} \\ \lambda^{-1}\sqrt{T_0}\,C_1^\lambda \end{pmatrix}(t) \,-\, \exp\left(-\frac{t}{\lambda}J\right)\cdot \begin{pmatrix} E^\lambda - E^\lambda_{\text{slow}} \\ \lambda^{-1}\sqrt{T_0}\,C_1^\lambda \end{pmatrix}(t=0)\,,
$$

where $\exp(tJ)$ is the rotation matrix given by (1.12). The vector $\mathbf{U}^\lambda$ vanishes at $t=0$ while it satisfies the following equation

$$
(2.9)\qquad \partial_t \mathbf{U}^\lambda \,+\, \frac{1}{\lambda}\,J\cdot\mathbf{U}^\lambda \,+\, \mathbf{S}^\lambda \,=\, 0\,.
$$

Multiplying (2.9) by $\exp(tJ/\lambda)$ and integrating in time, we obtain the following Duhamel formula

$$
(2.10)\qquad \mathbf{U}^\lambda(t) \,=\, -\int_0^t \exp\left(\frac{s-t}{\lambda}J\right)\cdot \mathbf{S}^\lambda(s)\,\mathrm{d}s\,, \qquad \forall t\geq 0\,.
$$

In Proposition 2.1 below we prove that if (1.9) is satisfied, the remainder in the former Duhamel formula may be neglected as $\lambda\to 0$, which leads to the asymptotic expansion (1.13). This result ensures that the field E^λ and the flux C_1^λ converge to the quasineutral limit up to bounded time oscillations around the quasineutral state.

In the Hermite framework, the formalization of condition (1.9) translates in the following statement: there exists $0\leq\alpha<1$ and a final time $T>0$ such that

$$
(2.11)\qquad \sup_{0<\lambda<1}\left(\lambda^{\alpha-1}\left\|C_1^\lambda(0)\right\|_{W^{r_0+1,4}(\mathbb{T})} \,+\, \sup_{t\in[0,T]}\lambda^\alpha\left\|E^\lambda(t)\right\|_{W^{r_0+2,4}(\mathbb{T})}\right) \,<\, +\infty\,,
$$

where $r_0 = \lceil 1/(1-\alpha)\rceil$, $\lceil\cdot\rceil$ denotes the upper integer part and where $W^{r_0,4}$ is the Sobolev space of order r_0 based on L^4. Furthermore, we assume that

$$
(2.12)\qquad \sup_{0<\lambda<1}\,\sup_{t\in[0,T]}\,\max_{k\leq 4}\left\|C_k^\lambda(t)\right\|_{W^{r_0+3,4}(\mathbb{T})} \,<\, +\infty\,,
$$

meaning that the solution to the Vlasov-Poisson system remains uniformly regular with respect to λ. Thus, under the latter two hypothesis, we are able to prove that the formal expansion (1.13) holds true with optimal convergence rates in λ. To that aim, we define the following distances

$$\left\{\begin{aligned} \mathcal{E}_0^\lambda(t) &:= \left\|E^\lambda(t) - E^\lambda_{\text{slow}}(t) - E^\lambda_{\text{osc}}(t)\right\|_{L^2(\mathbb{T})}, \\ \mathcal{E}_1^\lambda(t) &:= \left\|C_1^\lambda(t) - C^\lambda_{1,\text{osc}}(t)\right\|_{L^2(\mathbb{T})}, \end{aligned}\right. \tag{2.13}$$

where we decompose the electric field into two parts, namely the quasineutral state and its oscillating counterpart, and the same for the current density C_1^λ. These oscillating quantities read

$$\left\{\begin{aligned} E^\lambda_{\text{osc}}(t,x) &:= \cos\left(\frac{t}{\lambda}\right)\left(E^\lambda - E^\lambda_{\text{slow}}\right)(0,x) - \frac{\sqrt{T_0}}{\lambda}\sin\left(\frac{t}{\lambda}\right) C_1^\lambda(0,x), \\ C^\lambda_{1,\text{osc}}(t,x) &:= \cos\left(\frac{t}{\lambda}\right) C_1^\lambda(0,x) + \frac{\lambda}{\sqrt{T_0}}\sin\left(\frac{t}{\lambda}\right)\left(E^\lambda - E^\lambda_{\text{slow}}\right)(0,x). \end{aligned}\right. \tag{2.14}$$

We are now able to prove the following result.

Proposition 2.1. *Consider a family of solutions $(C^\lambda, \phi^\lambda)_{\lambda>0}$ to (2.5) with zero total flux*

$$\int_{\mathbb{T}} C_1^\lambda(t,x)\,\mathrm{d}x = 0,$$

and global mass $|\mathbb{T}|$. Suppose that they satisfy the compatibility assumption (2.11) and the uniform regularity assumption (2.12), for some given final time $T > 0$. Then, for all $t \in [0,T]$, and all $0 < \lambda < 1$, the following bounds hold for the electric field and the flux (E^λ, C_1^λ):

$$\mathcal{E}_0^\lambda(t) \le C\,\lambda^{1-\alpha} \qquad \text{and} \qquad \mathcal{E}_1^\lambda(t) \le C\,\lambda^{2-\alpha},$$

where the constant C only depends on α, T, T_0, $|\mathbb{T}|$ and the implicit constants in (2.11)-(2.12).

Proof. The proof is postponed in Appendix A. □

Remark 2.2. *It is worth mentioning that our analysis does not cover the critical case $\alpha = 1$. Actually, in this critical case, the limit of f^λ is still valid up to a change of variable, however it is only possible to characterize the convergence of E^λ as*

$$\lambda\left(E^\lambda - E^\lambda_{\text{osc}}\right) \longrightarrow 0, \quad \textit{as} \quad \lambda \to 0,$$

which means that the slow part of E^λ remains not clearly identified, see [27, 28] for details.

3. Fully discrete scheme

In this section, we introduce the numerical scheme used to approximate the Vlasov–Poisson system recast in the Hermite framework (2.5) and we analyze its properties. We begin by discussing the discretization of the phase space $\mathbb{T}\times\mathbb{R}$ in Section 3.1. Then, in Section 3.2, we present a first-order time integration scheme based on operator splitting between linear and nonlinear terms. The theoretical properties of the proposed scheme are then analyzed in Section 3.3. Finally, Section 3.4 is devoted to the extension of the first-order method to higher-order accuracy in time. In particular, we propose a second-order time integration scheme based on Strang splitting, combined with an implicit Runge–Kutta method applied to each substep of the splitting.

3.1. Phase-space discretization.

To discretize the phase space domain, we fix a number of Hermite modes $N_H \in \mathbb{N}^*$. Then, we consider the interval (a,b) of $\mathbb{R}$ and for $N_x \in \mathbb{N}^\star$, we introduce the set $\mathcal{J} = \{1,\dots,N_x\}$ and a family of control volumes $(K_j)_{j\in\mathcal{J}}$ such that $K_j = \left]x_{j-1/2}, x_{j+1/2}\right[$ with x_j the middle of the interval K_j and

$$a = x_{1/2} < x_1 < x_{3/2} < \dots < x_{j-1/2} < x_j < x_{j+1/2} < \dots < x_{N_x} < x_{N_x+1/2} = b.$$

We also define the mesh sizes

$$\left\{\begin{aligned} &\Delta x_j = x_{j+1/2} - x_{j-1/2}, \ \text{ for } j \in \mathcal{J}, \\ &\Delta x_{j+1/2} = x_{j+1} - x_j, \ \text{ for } 1 \le j \le N_x - 1. \end{aligned}\right.$$

and the parameter h such that

$$h = \max_{j\in\mathcal{J}} \Delta x_j .$$

We then introduce the discrete operator $\partial_h = (\partial_j)_{j\in\mathcal{J}}$ representing the centered finite volume approximation of ∂_x given by

$$\partial_j C = \frac{\mathcal{C}_{j+1} - \mathcal{C}_{j-1}}{2\Delta x_j}, \quad j \in \mathcal{J}, \tag{3.1}$$

for all $C = (\mathcal{C}_j)_{j\in\mathcal{J}}$. The above detailed choices lead to the following semi-discrete system

$$\begin{cases} \dfrac{\mathrm{d}C_k}{\mathrm{d}t} + \sqrt{k\,T_0}\,\partial_h C_{k-1} + \sqrt{(k+1)\,T_0}\,\partial_h C_{k+1} - \sqrt{\dfrac{k}{T_0}}\,E\,C_{k-1} = 0, \\ E = -\partial_h \phi\,; \quad -\lambda^2 \partial_h^2 \phi = C_0 - 1, \end{cases} \tag{3.2}$$

for $k \in \{0, \ldots, N_H\}$ and $C_k = 0$ when $k > N_H$ and $k = -1$. System (3.2) is then completed with the condition

$$\sum_{j\in\mathcal{J}} \Delta x_j\, \phi_j = 0,$$

ensuring uniqueness of the discrete potential $(\phi_j)_{j\in\mathcal{J}}$.

3.2. **First order time splitting scheme.** The time discretization is based on a time splitting technique, where the first step consists in solving the Vlasov-Poisson system, linearized around a quasineutral steady state $C^{\mathrm{stat}} = (\delta_{0,k})_{k\in\mathbb{N}}$. The second step, consists in solving the remaining nonlinear part of the system. More precisely, we first rewrite the semi-discrete system (3.2) as

$$\frac{\mathrm{d}C_k}{\mathrm{d}t} + \mathcal{L}_k\, C + \mathcal{B}_k(C) = 0, \tag{3.3}$$

for each $k \in \{0, \ldots, N_H\}$. We separate the contribution of the linear operator $\mathcal{L} = (\mathcal{L}_k)_{0\le k\le N_H}$ from that of the nonlinear operator $\mathcal{B} = (\mathcal{B}_k)_{0\le k\le N_H}$. The first discrete operator is defined for the modes $C = (C_k)_{0\le k\le N_H}$ as

$$\mathcal{L}_k\, C = \sqrt{k\,T_0}\,\partial_h C_{k-1} + \sqrt{(k+1)T_0}\,\partial_h C_{k+1}, \quad \text{for } k \neq 1,$$

with $C_k = 0$ when $k > N_H$ and $k = -1$ and

$$\mathcal{L}_1\, C = \sqrt{T_0}\,\partial_h C_0 + \sqrt{2\,T_0}\,\partial_h C_2 - \frac{1}{\sqrt{T_0}}\,E, \quad \text{with} \quad E = -\partial_h\phi, \quad \text{and} \quad -\lambda^2\partial_h^2\phi = C_0 - 1.$$

The second nonlinear operator $\mathcal{B} = (\mathcal{B}_k)_{0\le k\le N_H}$ is defined by

$$\begin{cases} \mathcal{B}_0(C) = 0, \\ \mathcal{B}_k(C) = -\sqrt{\dfrac{k}{T_0}}\,E\,(C_{k-1} - \delta_{1,k}), \quad \text{if } k \ge 1, \\ E = -\partial_h\phi, \quad \text{and} \quad -\lambda^2\partial_h^2\phi = C_0 - 1, \end{cases}$$

where $\delta_{1,k}$ denotes the Kronecker symbol. We then fix a time step $\Delta t > 0$, set $t^n = n\Delta t$ with $n \in \mathbb{N}$, and solve first the linear part on $[t^n, t^{n+1}]$ with a first order fully implicit Euler scheme. This yields the following linear system to invert

$$\begin{cases} \dfrac{C_1^{(1)} - C_1^n}{\Delta t} + \sqrt{T_0}\,\partial_h C_0^{(1)} + \sqrt{2\,T_0}\,\partial_h C_2^{(1)} - \dfrac{1}{\sqrt{T_0}}\,E^{(1)} = 0, \\ \dfrac{C_k^{(1)} - C_k^n}{\Delta t} + \sqrt{k\,T_0}\,\partial_h C_{k-1}^{(1)} + \sqrt{(k+1)T_0}\,\partial_h C_{k+1}^{(1)} = 0, \quad \text{for } k \neq 1, \\ E^{(1)} = -\partial_h\phi^{(1)}\,; \quad -\lambda^2\partial_h^2\phi^{(1)} = C_0^{(1)} - 1, \end{cases} \tag{3.4}$$

where $C^{(1)}$ indicates the solution obtained after this first splitting-step for $k \in \{0, \ldots, N_H\}$ and, as before, with $C_k^{(1)} = 0$ when $k > N_H$ and $k = -1$. To the above system (3.4), we add the following uniqueness condition

$$\sum_{j\in\mathcal{J}} \Delta x_j\, \phi_j^{(1)} = 0.$$

Let us observe that equations (3.4) can be recast in matrix-vector form, where the coefficients of the unknowns are independent of the time index n. Therefore, one can perform an LU factorization of the system at $n = 0$ and store the resulting LU factors to be reused for all $n \geq 0$ improving computational efficiency. We now focus on the second part of the splitting which involves the nonlinear operator $\mathcal{B}$. This corresponds to

$$\left\{ \begin{aligned} &\frac{\mathrm{d}C_k}{\mathrm{d}t} + \mathcal{B}_k(C) = 0\,, \\ &C(t^n) = C^{(1)}\,. \end{aligned} \right.$$

We approximate the above system by using again a fully implicit Euler scheme. This reads

$$\left\{ \begin{aligned} &C_0^{n+1} = C_0^{(1)}\,, \\ &E^{n+1} = E^{(1)}\,, \\ &\frac{C_k^{n+1} - C_k^{(1)}}{\Delta t} - \sqrt{\frac{k}{T_0}}\, E^{n+1} \left(C_{k-1}^{n+1} - \delta_{k,1} \right) = 0\,, \quad \text{if } k \geq 1\,, \end{aligned} \right. \tag{3.5}$$

for $k \in \{0, \ldots, N_H\}$ and $C_k^{n+1} = 0$ when $k > N_H$. Observe that since the electric field $E^{(1)}$ and the density $C_0^{(1)}$ do not change during this second step, the latter system is trivially invertible and hence does not require any particular linear solver. As opposite to previous methods, the novelty of the approach proposed lies in discretizing the Poisson equation simultaneously with the equations governing the Hermite coefficients $(C_k)_{0 \leq k \leq N}$, as done in [6, 4]. Let in fact observe that the strategy above discussed differs from other recent approaches that reformulate the Poisson equation as a harmonic oscillator-type equation for the potential ϕ, and then build a numerical scheme based on that reformulation (see, for instance, [13, 3, 1, 18, 19, 14, 17]). In contrast, our method retains the original structure of the Vlasov–Poisson system. However, as we explain later in Proposition 3.3, it is still possible to recover a harmonic oscillator formulation for the electric potential from the system (3.4)–(3.5) as done in previous works. Ultimately, we emphasize the importance of solving the coefficients (C_0, C_1, ϕ) in a completely implicit manner, as they exhibit fast oscillations in the quasineutral regime and so introducing a stiffness into the equations.

3.3. **Discrete quasineutral limit.** In this section, we investigate the theoretical properties of the numerical method (3.4)–(3.5). In Proposition 3.1, we show that the proposed scheme provides a consistent discretization of the quasineutral limit for fixed time step Δt. In addition to this result, in Proposition 3.3, we demonstrate that the proposed numerical method naturally encodes the harmonic oscillator reformulation of the Poisson equation.

We start by proving that a discrete counterpart of Proposition 2.1 holds true with however a fundamental difference: the numerical scheme (3.4)–(3.5) filter out the oscillations when the parameters $\lambda \to 0$ and Δt is fixed. This is mainly due to the dissipative nature of implicit scheme. In more detail, we prove that, for fixed Δt and under a discrete version of the compatibility condition (2.11), the numerical method (3.4)–(3.5) consistently approximates the quasineutral limit in the sense that:

$$E^n \underset{\lambda \to 0}{=} \sqrt{2}\, T_0\, \partial_h\, C_2^n + O(\lambda)\,, \quad \text{and} \quad C_1^n \underset{\lambda \to 0}{=} O(\lambda)\,.$$

To state our result, we use the discrete L^2 and H^r norms of $C = (\mathcal{C}_j)_{j \in \mathcal{J}}$, defined as

$$\|C\|_{l^2(\mathcal{J})}^2 = \sum_{j \in \mathcal{J}} |\mathcal{C}_j|^2\, \Delta x_j\,, \quad \text{and} \quad \|C\|_{h^r(\mathcal{J})}^2 = \sum_{0 \leq s \leq r} \|\partial_h^s C\|_{l^2(\mathcal{J})}^2\,.$$

We also introduce the discrete analog of $\mathcal{E}_0$ and $\mathcal{E}_1$ of Proposition 2.1 in which however we remove the oscillatory part of the solution. They read

$$\left\{ \begin{aligned} &\mathcal{E}_0^n := \left\| E^n - \sqrt{2}\, T_0\, \partial_h\, C_2^n \right\|_{L^2(\mathcal{J})}\,, \\ &\mathcal{E}_1^n := \|C_1^n\|_{h^1(\mathcal{J})}\,. \end{aligned} \right. \tag{3.6}$$

We are now ready to prove the following result.

Proposition 3.1. *Let consider for a fixed* $\Delta t > 0$ *a solution* $(C^n, \phi^n)_{n\geq 0}$ *to* (3.4)-(3.5) *with zero total flux and with total mass* $|b-a|$, *that is*

$$\sum_{j\in\mathcal{J}} \mathcal{C}^0_{1,j}\,\Delta x_j \;= 0\,, \quad \text{and} \quad \sum_{j\in\mathcal{J}} \mathcal{C}^0_{0,j}\,\Delta x_j \;= |b-a|\,. \tag{3.7}$$

Suppose furthermore that $(C^n, \phi^n)_{n\geq 0}$ *satisfies the discrete analog of* (2.11) *with* $\alpha = 1$, *that is*

$$\sup_{\lambda>0}\ \sup_{0\leq n\leq T/\Delta t} \left(\|C^n_1\|_{h^1(\mathcal{J})} + \lambda\,\|E^n\|_{h^3(\mathcal{J})}\right) < +\infty\,, \tag{3.8}$$

for some given final time $T > 0$, *and that the discrete analog of* (2.12) *is satisfied, that is*

$$\sup_{0<\lambda}\ \sup_{0\leq n\leq T/\Delta t} \sum_{2\leq k\leq N_H} \|C^n_k\|^2_{h^2(\mathcal{J})} \;< +\infty\,. \tag{3.9}$$

In addition, suppose that the spatial mesh satisfies the following regularity constraint

$$\sup_{\lambda>0}\ \sup_{(i,j)\in\mathcal{J}^2} \Delta x_i/\Delta x_j \;<\; +\infty\,. \tag{3.10}$$

Then, we have for all $\lambda > 0$

$$\sup_{1\leq n\leq T/\Delta t} \mathcal{E}^n_0 \;\leq\; C\lambda\,, \quad \text{and} \quad \sup_{2\leq n\leq T/\Delta t} \mathcal{E}^n_1 \;\leq\; C\lambda\,, \tag{3.11}$$

where $C > 0$ *depends on* Δt *and on the implicit constants in* (3.8)-(3.9) *and* (3.10). *Furthermore, the constant* C *is uniform with respect to* λ *and the phase-space discretization parameters* $h > 0$ *and* $N_H \geq 2$.

The proof is detailed in Appendix B. The key point consist in proving that for $\Delta t > 0$ the scheme (3.4)-(3.5) filtrates the fast oscillations of E^n and C^n_1 around the quasineutral state. This permits to show that the sizes of E^n and C^n_1, prescribed by (3.8), are reduced by a factor λ for all $n \geq 1$. The main mathematical difficulty of the proof arises in the analysis of the nonlinear step (3.5). This requires the use of the discrete Sobolev injection $h^1(\mathcal{J}) \hookrightarrow l^\infty(\mathcal{J})$.

Remark 3.2. *We emphasize that our result remains valid also in the critical case* $\alpha = 1$, *which was not treated in the continuous setting in Section 2.2. In this critical case, the work* [27] *shows that* f^λ *converges to the quasi-neutral limit up to an oscillating component. The proposed numerical method filters this component and the numerical solution converges to the quasineutral limit directly.*

As already mentioned, recently proposed numerical methods addressing the quasineutrality issue uses to reformulate the Poisson equation as a harmonic oscillator equation. In the continuous Hermite framework, this reformulated Poisson equation can be derived by differentiating the potential equation (second line of (2.5)) twice in time and eliminating C^λ_0 and C^λ_1 using their corresponding evolution equations (first line of (2.5) for $k = 0$ and 1). These computations lead to the so-called reformulated Poisson equation:

$$\lambda^2\,\partial^2_t(\partial_x E^\lambda) + \partial_x(C^\lambda_0\,E^\lambda) = \partial^2_x(\sqrt{2}\,T_0\,C^\lambda_2 + T_0\,C^\lambda_0)\,. \tag{3.12}$$

It is then natural to ask whether an analogous discrete reformulated Poisson equation from to the proposed scheme can be obtained in our setting. This is the object of the following result.

Proposition 3.3. *Let* $(C^n)_{n\geq 0}$ *be a solution to* (3.4)-(3.5) *with* $E = -\partial_h\phi$, *then the following reformulated discrete Poisson equation for all* $n \geq 1$ *holds true:*

$$\begin{aligned}
&\lambda^2\,\frac{\partial_h E^{n+1} - 2\,\partial_h E^n + \partial_h E^{n-1}}{\Delta t^2} + \partial_h\left(E^{n+1}\,C^{n+1}_0\right)\\
&\quad = \partial^2_h\left(\sqrt{2}\,T_0\,C^{(1,n+1)}_2 + T_0\,C^{n+1}_0\right) + \lambda^2\,\Delta t\,\partial_h\left(\frac{E^{n+1}\,\partial_h E^{n+1} - E^n\,\partial_h E^n}{\Delta t}\right),
\end{aligned} \tag{3.13}$$

where $C^{(1,n+1)}_2$ *corresponds to the Hermite coefficient* $C^{(1)}_2$ *computed during the Step 1 of the time splitting scheme to get* $(C^{n+1}_k)_{k,\geq 0}$ *from* $(C^n_k)_{k\geq 0}$.

The proof is postponed in Appendix C.

3.4. **Second order time splitting scheme.** In this section, we extend the first-order time method described in (3.4)–(3.5) to a second-order discretization. To this end, observe that each step of the time-splitting scheme (3.4)–(3.5) consists of a first-order implicit method. Therefore, this approach can be generalized to higher-order schemes by employing existing Runge–Kutta techniques [9, 31]. In particular, we apply a second-order time-splitting strategy (Strang splitting), combined with a second-order stiffly accurate implicit Runge–Kutta method. Thus, given the equation

$$\frac{\mathrm{d}C_k}{\mathrm{d}t} + \mathcal{L}_k C + \mathcal{B}_k(C) = 0\,, \tag{3.14}$$

for all coefficients $k \in \{0, \ldots, N_H\}$ of the Hermite expansion, we proceed as follows. For each time step starting from C^n, we first solve the linear part on half time step $\Delta t/2$ by taking as initial data $C^{(0)} = C^n$:

$$\frac{\mathrm{d}C_k}{\mathrm{d}t} + \mathcal{L}_k C = 0,$$

for all coefficients $k \in \{0, \ldots, N_H\}$. We set $C^{(1)}$ the solution obtained after this half time step and then we solve the nonlinear part on a full time step Δt using $C^{(1)}$ as initial data. This reads

$$\frac{\mathrm{d}C_k}{\mathrm{d}t} + \mathcal{B}_k(C) = 0\,.$$

Finally, by setting $C^{(2)}$ the solution obtained after this second step as a new initial data, we conclude the splitting procedure by solving the linear part on another half time step $\Delta t/2$:

$$\frac{\mathrm{d}C_k}{\mathrm{d}t} + \mathcal{L}_k C = 0.$$

This gives $C^{(3)} = C^{n+1}$ The solution at time t^{n+1}. Moreover, each of the substeps above is solved using a second-order, fully implicit, stiffly accurate Runge–Kutta scheme, defined as follows:

$$\begin{cases} K_1 \;=\; \mathcal{F}\left(C^{(i)} - \gamma\,\overline{\Delta t}\,K_1\right), \\[2mm] K_2 \;=\; \mathcal{F}\left(C^{(i)} - (1-\gamma)\,\overline{\Delta t}\,K_1 - \gamma\,\overline{\Delta t}\,K_2\right), \\[2mm] C^{(i+1)} \;=\; C^{(i)} \;-\; (1-\gamma)\,\overline{\Delta t}\,K_1 \;-\; \gamma\,\overline{\Delta t}\,K_2\,, \end{cases}$$

where $\mathcal{F} \in \{\mathcal{L}, \mathcal{B}\}$, $\gamma = 1 - \frac{1}{\sqrt{2}}$, and $\overline{\Delta t}$ denotes Δt in the case of the nonlinear component and $\Delta t/2$ in the case of the two half-steps for the linear component. Finally the superscripts (i) and (i+1) indicate respectively the value of the Hermite coefficients at the beginning and at the end of the Strang splitting substep.

4. Numerical simulations

The numerical experiments are conducted using the second order method presented in the previous Section 3.4. The temperature T_0 is fixed to $T_0 = 1$ for all tests, if not otherwise stated, while the other numerical parameters are chosen based on the specific test case and made precise in the rest of the section, in order to accurately capture the physical phenomena under investigation.

4.1. **Near equilibrium.** We first consider an initial distribution for the Vlasov–Poisson system (1.3), consisting of a perturbation from a global Maxwellian state of order $\delta\lambda^{2-\alpha}$, with $\alpha \in [0, 1)$, given by

$$f^{\lambda}_{\mathrm{in}}(x, v) \;=\; \frac{1}{\sqrt{2\pi}}\,\left(1 + \delta\lambda^{2-\alpha}\cos\left(k_x x\right)\right)\exp\left(-\frac{|v|^2}{2}\right)\,. \tag{4.1}$$

The spatial domain is $x \in [-10, 10]$, the frequency $k_x = \pi/10$ while we fix the size of the perturbation to $\delta = 0.1$. A reference solution is computed to assess the numerical order of convergence of the quantities $\mathcal{E}^{\lambda}_0$ and $\mathcal{E}^{\lambda}_1$, defined in (2.13)-(2.14), describing the oscillatory components of the electric field E^{λ} and C^{λ}_1, respectively. This solution uses $N_H = 128$ Hermite modes, $N_x = 2048$ mesh points in the physical space and $\Delta t = 10^{-4}$ chosen to resolve the smallest value of the Debye length, $\lambda = 10^{-2}$ considered in the simulations. As shown in [28], for this class of initial data with $\alpha \in [0, 1)$, the quantities $(f^{\lambda}, E^{\lambda})$ converge weakly to its quasi neutral limit (f^0, E^0) as $\lambda \to 0$, where:

$$f^0(v) \;=\; \frac{1}{\sqrt{2\pi}}\,\exp\left(-\frac{|v|^2}{2}\right),\;\; E^0 = 0, \tag{4.2}$$

which corresponds to the stationary solution of the quasi-neutral model (1.7).

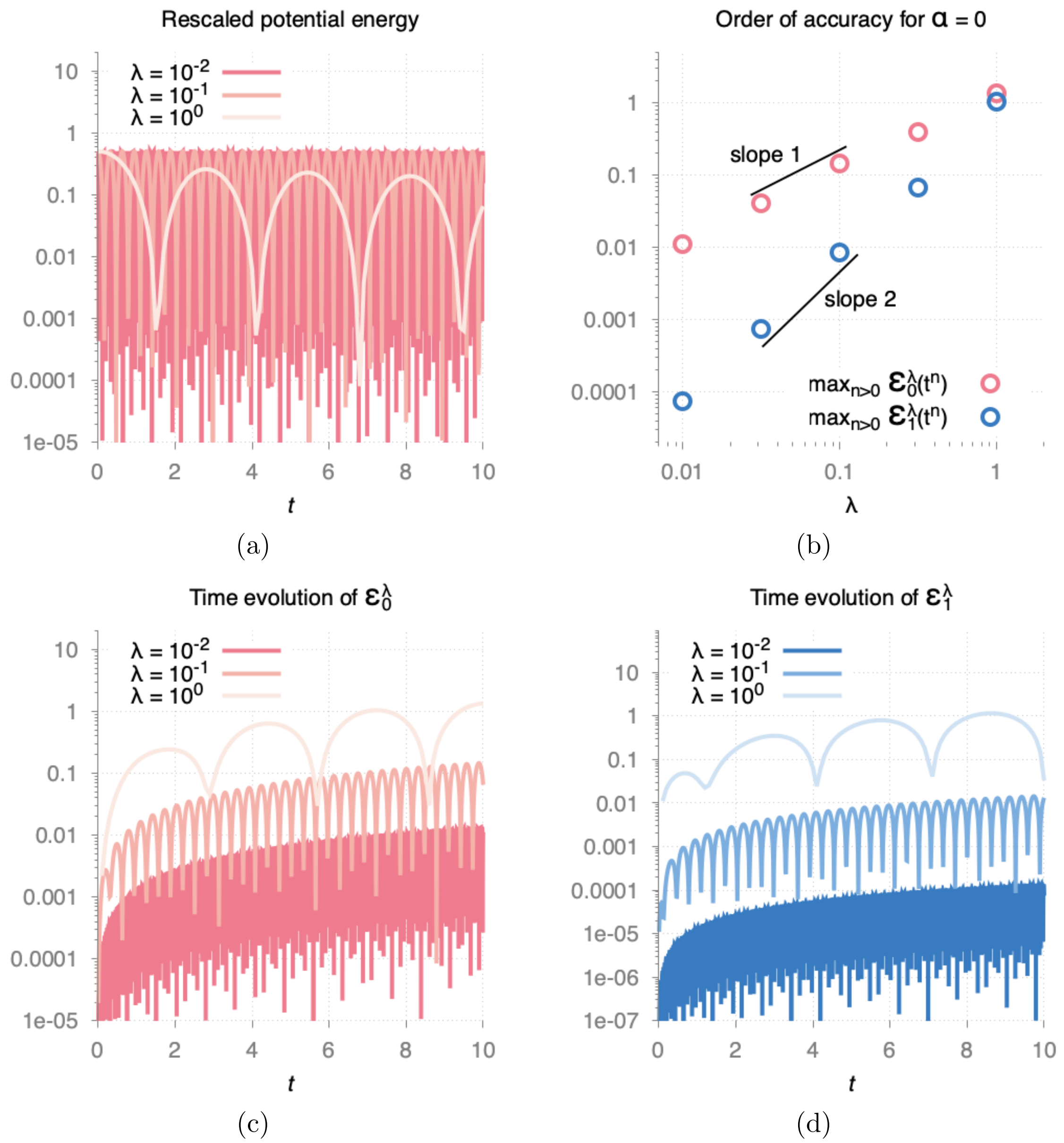

FIGURE 4.1. **Near equilibrium test case with** $\alpha = 0$ **:** (a) time evolution of the rescaled potential energy $\frac{1}{2}\sum_{j\in\mathcal{J}}\Delta x_j\,|E_j^n|^2$; (b) order of convergence for $\max_{n\geq 0}\mathcal{E}_0^\lambda(t^n)$ and $\max_{n\geq 0}\mathcal{E}_1^\lambda(t^n)$; (c) time evolution of $\mathcal{E}_0^\lambda(t)$ and (*d*) time evolution of $\mathcal{E}_1^\lambda(t)$, as defined in (2.13)-(2.14), for different values of λ.

In Figure 4.1-(a) the time evolution of the rescaled potential energy

$$\frac{1}{2}\sum_{j\in\mathcal{J}}\Delta x_j\,|E_j^n|^2\,,$$

is shown in the case $\alpha = 0$. The oscillatory nature of the electric field with a frequency inversely proportional to λ appears clear. Figure 4.1-(b) shows instead the quantities

$$\max_{n\geq 0}\mathcal{E}_0^\lambda(t^n) \qquad \text{and} \qquad \max_{n\geq 0}\mathcal{E}_1^\lambda(t^n)\,,$$

confirming that the expected order of convergence established in Proposition 2.1 is obtained. Moreover, these results indicate that the solution E^λ converges to its quasi-neutral limit E^0 up to the fast time oscillations explicitly characterized by the initial condition (2.14).

Figure 4.2 show the same quantities as Figure 4.1, in the case of $\alpha = 1/2$. We observe that, as predicted by the theory, the amplitude of the electric field is now of order $O(\lambda^{-1/2})$ as λ approaches zero (Figure 4.2-(a)). Our numerical simulations confirm the results of Proposition 2.1: oscillation frequency in time

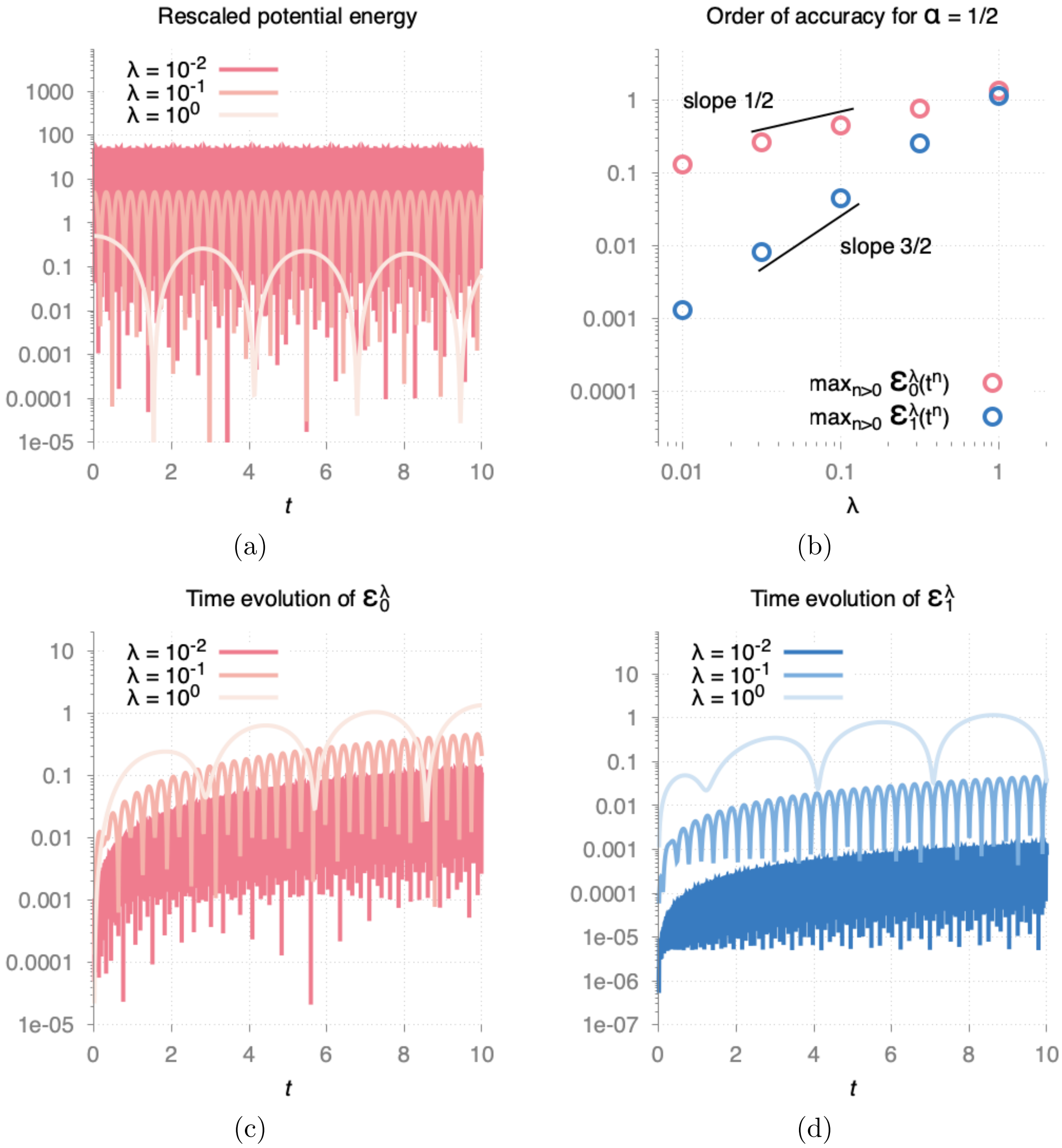

FIGURE 4.2. **Near equilibrium test case with $\alpha = 1/2$:** (a) time evolution of the rescaled potential energy $\frac{1}{2}\sum_{j\in\mathcal{J}} \Delta x_j\, |E_j^n|^2$; (b) order of convergence for $\max_{n\geq 0} \mathcal{E}_0^\lambda(t^n)$ and $\max_{n\geq 0} \mathcal{E}_1^\lambda(t^n)$; (c) time evolution of $\mathcal{E}_0^\lambda(t)$ and (d) time evolution of $\mathcal{E}_1^\lambda(t)$, as defined in (2.13)-(2.14), for different values of λ.

and order of convergence for $\mathcal{E}_0^\lambda$ and $\mathcal{E}_1^\lambda$ are retrieved (Figure 4.2-(b)). Let us also observe that, while the norm of E^λ grows as $\lambda \to 0$, the electric field E^λ strongly converges to its quasineutral limit E^0 up to explicitly known fast oscillations in time.

We then consider the case $\alpha = 1$. This situation lies outside the scope of our theoretical analysis. Nevertheless, this test allows to assess the limit of the numerical scheme proposed. The results are shown in Figure 4.3. The amplitude of the electric field is now of order $O(\lambda^{-1})$ while $\max_{n\geq 0} \mathcal{E}_0^\lambda(t^n)$ no longer converges to zero as $\lambda \to 0$ (Figure 4.3-(b) and (c)). This confirms the theoretical investigations [27, 28], which show that $\lambda\,\mathcal{E}_0^\lambda \to 0$. In contrast, the quantity $\mathcal{E}_1^\lambda$ remains of order λ (Figure 4.3-(b) and (d)) suggesting that Proposition 2.1 may remain true even with $\alpha = 1$.

Finally, we investigate the behavior of our numerical scheme when the time step Δt and the space mesh size are fixed while the quasineutral parameter λ tends to zero. The aim is to study the ability of the scheme to capture the correct asymptotic behavior. The numerical parameters are $\Delta t = 0.2$, $N_x = 64$ and $N_H = 128$. In Figure 4.4, the results are presented for $\alpha = 0$ and $\alpha = 1/2$ indicating that time evolution of the potential energy, amplitude and frequency, is in line with the theoretical findings even for a large time step $\Delta t = 0.2$ (Figure 4.4-(a) and (b)). However, when λ becomes smaller ($\lambda = 10^{-2}$ and 10^{-3}), these discretization parameters are no longer sufficient to describe the small time scales. Hence, the electric field

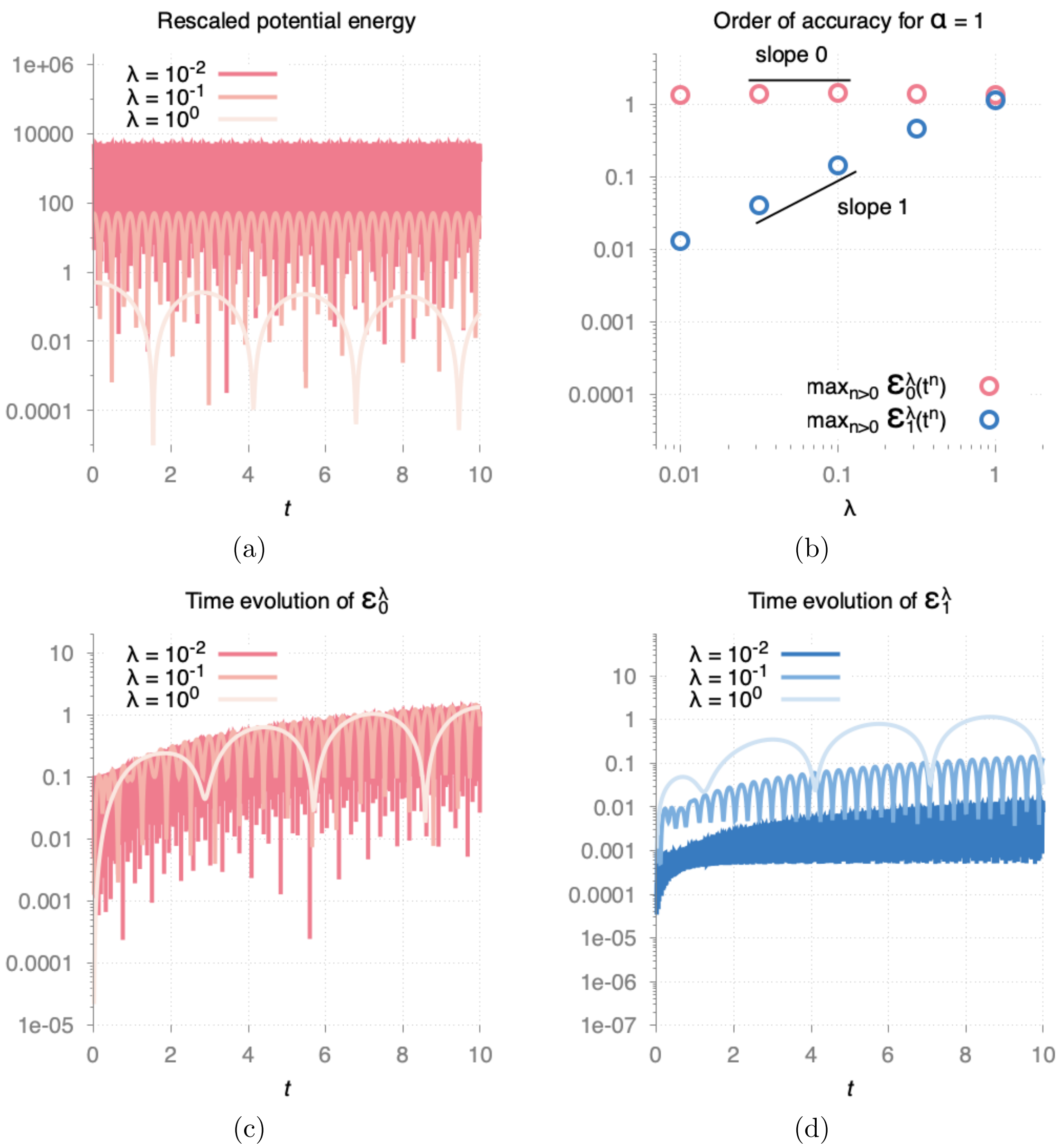

FIGURE 4.3. **Near equilibrium test case with $\alpha = 1$:** (a) time evolution of the rescaled potential energy $\frac{1}{2}\sum_{j\in\mathcal{J}} \Delta x_j \, |E_j^n|^2$; (b) order of convergence for $\max_{n\geq 0} \mathcal{E}_0^\lambda(t^n)$ and $\max_{n\geq 0} \mathcal{E}_1^\lambda(t^n)$; (c) time evolution of $\mathcal{E}_0^\lambda(t)$ and (d) time evolution of $\mathcal{E}_1^\lambda(t)$, as defined in (2.13)-(2.14), for different values of λ.

converges toward the expected weak limit. For the case $\alpha = 1$, where the results of Proposition 2.1 are no longer valid, we observe that, for $\lambda = 10^{-1}$ and 10^{-2} (Figure 4.4-(c)), the numerical solution becomes unstable and blows-up. This demonstrates that in such cases, time step and spatial mesh need to be refined to obtain stable results. This lack of uniform stability should not be interpreted as a limit of the scheme, since in this case Proposition 3.1 does not apply. It is interesting to notice that, for $\lambda = 10^{-3}$ and $\Delta t = 0.2$, the scheme regains stability and the rescaled potential energy is instantaneously damped, which means that the electric field E^λ converges to zero.

4.2. **Smooth perturbation of equilibrium.** We now consider an initial distribution with non homogeneous temperature driven by a perturbation of order $O(1)$ as $\lambda \to 0$. This reads

$$f_{\rm in}(x,v) \;=\; \frac{1}{\sqrt{2\pi\, T_{\rm in}(x)}} \exp\left(-\frac{|v|^2}{2\, T_{\rm in}(x)}\right), \tag{4.3}$$

with $x \in [-10, 10]$, frequency $k_x = \pi/10$ and $T_{\rm in}$ given by

$$T_{\rm in}(x) = 1 + \delta \, \cos\left(k_x x\right).$$

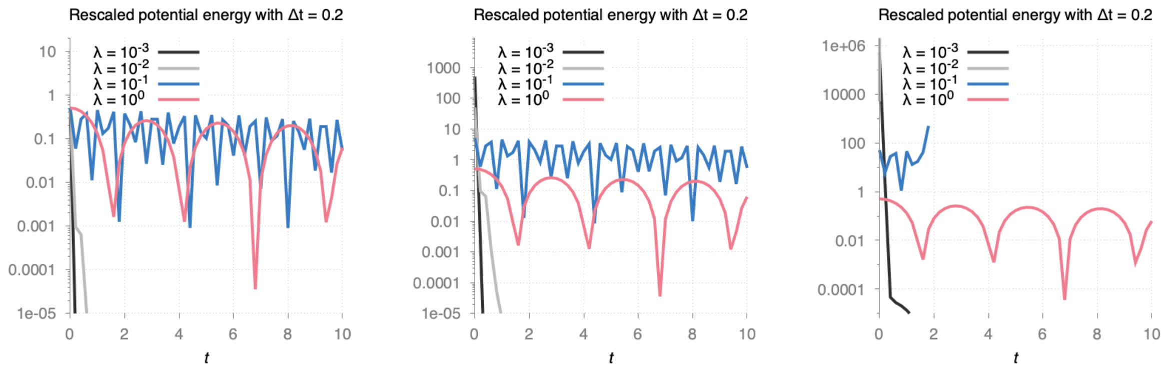

(a) $\alpha = 0$ (b) $\alpha = 1/2$ (c) $\alpha = 1$

FIGURE 4.4. **Near equilibrium test case.** Time evolution of the rescaled potential energy $\frac{1}{2}\sum_{j\in\mathcal{J}} \Delta x_j\, |E_j^n|^2$ with $\Delta t = 0.2$, $N_x = 64$ and $N_H = 128$ for different λ: (a) $\alpha = 0$; (b) $\alpha = 1/2$; (c) $\alpha = 1$.

This gives for the density and the flux the following relations

$$\rho_{\text{in}}(x) = \int_{\mathbb{R}} f_{\text{in}}(x,v)\mathrm{d}v \;=\; 1 \quad \text{and} \quad j_{\text{in}}(x) = \int_{\mathbb{R}} f_{\text{in}}(x,v)v\,\mathrm{d}v \;=\; 0\,, \qquad \forall x \in (-10,10)\,.$$

In this situation, the quasineutral model (1.7) has a non trivial slow dynamics in time that we wish to describe using the proposed numerical approximation. The reference solution is obtained using the second order scheme 3.4 with a fine mesh, $N_H = 2000$, $N_x = 1000$ and $\Delta t = 10^{-3}$, which permits to describe both the fast and the slow scales for different values of the Debye length, namely $\lambda \in \{1, 0.3, 0.1, 0.03\}$. The time evolution of the L^2 norm of the electric field E^λ and the slow component $E^\lambda_{\text{slow}} = \sqrt{2}\partial_x C_2^\lambda$ are shown in Figure 4.5 and in Figure 4.6 respectively (red curves). When $\lambda = 1$, a damping of the electric field is observed as opposite to the case $\lambda \ll 1$, where the electric field oscillates with a frequency inversely proportional to the Debye length λ. At the same time, the slow component E^λ_{slow} is first strongly damped, then it oscillates slowly (independently of λ) and finally, when its amplitude is in order of $\delta\lambda^2$, it starts to oscillate rapidly with a frequency inversely proportional to λ. The observed results stay in good agreement with the analytical investigations of [27, 8].

In Figures 4.5 and 4.6, the accuracy and robustness of the second order scheme for a wide range of λ is measured using $N_x = 100$, $\Delta t = 0.2$, $N_H = 400$ with different values of the Debye length $\lambda \in \{1,\,10^{-1},\,10^{-2},\,10^{-3}\}$. The numerical results show both the time evolution of the L^2 norm of the electric field E^λ and its slow counterpart E^λ_{slow}. When λ and Δt are of the same order, the discrete system is not stiff and a coarse mesh allows to describe precisely the time oscillations as seen in Figures 4.5 and 4.6 (a)-(b). When λ assumes smaller values, the time step $\Delta t = 0.2$ becomes too large to provide a good approximation of the fast scales as one can notice in Figures 4.5 and 4.6 (c)-(d). However, from Figure 4.6-(c), one can observe that, in the case in which the norm of E^λ_{slow} is greater than the threshold $\delta\,\lambda^2$, the numerical scheme is still able to describe correctly the slow scale dynamics of E^λ_{slow}. When $\lambda = 3\cdot 10^{-2}$, the numerical method eliminates the fast physical oscillations and projects the solution on the quasineutral slow dynamics limit, see Figures 4.5-(d) and 4.6-(d)). As illustration of the so-called asymptotic preserving property possessed by our method, it is worth mentioning that, when $\lambda \to 0$, the numerical scheme still captures the slow dynamics with a large time step, namely $\Delta t = 0.2$, see Figure 4.7.

In summary, the results discussed show, in the quasineutral regime, the stability and consistency of the numerical scheme (3.4)-(3.5) and of its second order counterpart without a prohibitive computational cost. A trade-off inherent of this approach is, however, the filtering of high-frequency oscillations.

4.3. **Oscillatory perturbation from equilibrium.** We consider now an oscillatory initial distribution f_{in}. This reads

$$f_{\text{in}}(x,v) \;=\; \frac{1}{\sqrt{2\pi\, T_{\text{in}}(x)}}\; (1 + \delta\cos(k_x x)\,\sin(3\pi\, v))\,\exp\left(-\frac{|v|^2}{2\,T_{\text{in}}(x)}\right)\,, \tag{4.4}$$

with $\delta = 0.05$, $x \in [-10, 10]$, $k_x = \pi/10$ and T_{in} given by

$$T_{\text{in}}(x) = 1 + \delta\,\cos\left(k_x x\right).$$

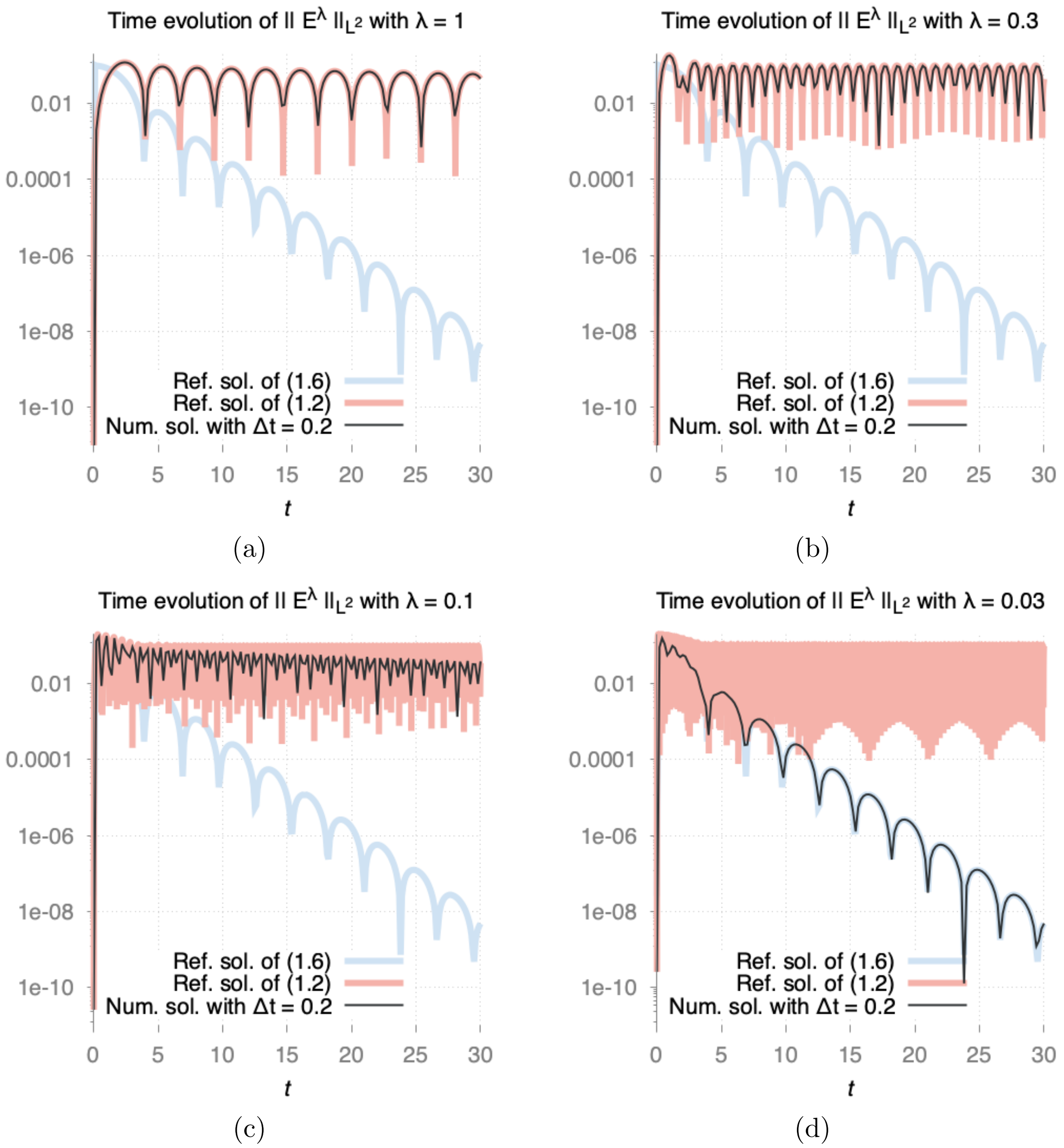

FIGURE 4.5. **Smooth perturbation of equilibrium test case:** time evolution of $\|E^\lambda\|_{L^2}$ in logarithmic scale with *(a)* $\lambda = 1$; *(b)* $\lambda = 3.\ 10^{-1}$; *(c)* $\lambda = 10^{-1}$ and *(d)* $\lambda = 3.10^{-2}$.

As for the previous test case, we have $\rho_{\text{in}}(x) = 1$ and $j_{\text{in}}(x) = 0$, while high order moments are not spatially homogeneous. The chosen configuration is such that the initial perturbation induces oscillations in the velocity space and, in this situation, one does not expect a fast convergence to zero of the slow component E^λ_{slow}. In fact, even in the quasineutral regime, velocity oscillations produce a sort of "echo" in the solution, so that the electric field exhibits slowly decaying oscillations with respect to time.

The reference solution is obtained using a fine mesh with $N_H = 1200$, $N_x = 500$, $\Delta t = 10^{-3}$ and the second order in time scheme presented in Section 3.4. This permits to capture both fast and slow scales phenomena for different values of the Debye length: $\lambda \in \{1, 10^{-1}, 10^{-2}, 10^{-3}\}$. In Figure 4.8 the time evolution of the L^2 norm of the electric field E^λ is shown while in Figure 4.9 is reported the slow component $E^\lambda_{\text{slow}} = \sqrt{2}\partial_x C^\lambda_2$. When $\lambda = 1$, the L^2 norm of the electric field is first damped and oscillates slowly, then, when $t \simeq 25$, the "echo" is observed. When $\lambda \ll 1$, the electric field E^λ_{osc} starts to oscillate with a frequency inversely proportional to λ, while the slow component $E^\lambda_{\text{slow}} = \sqrt{2}\,\partial_x C^\lambda_2$ is first strongly damped, then its amplitude increases again to reach a maximum around time $t \simeq 12.5$ and $t \simeq 25$ (see Figure 4.9). The fast oscillations of E^λ_{slow} have an amplitude of the order of $\delta\lambda^2$ (*cf.* Section 4.2) and they are not visible on Figure 4.9 since the amplitude of $\|\sqrt{2}\,\partial_x C^\lambda_2\|_{L^2}$ is above this threshold.

To investigate the asymptotic preserving property of the scheme we performed numerical simulations on a coarse mesh, namely $N_x = 100$, $\Delta t = 0.1$ and $N_H = 1200$ for a wide variety of $\lambda \ll 1$. Notice that, in

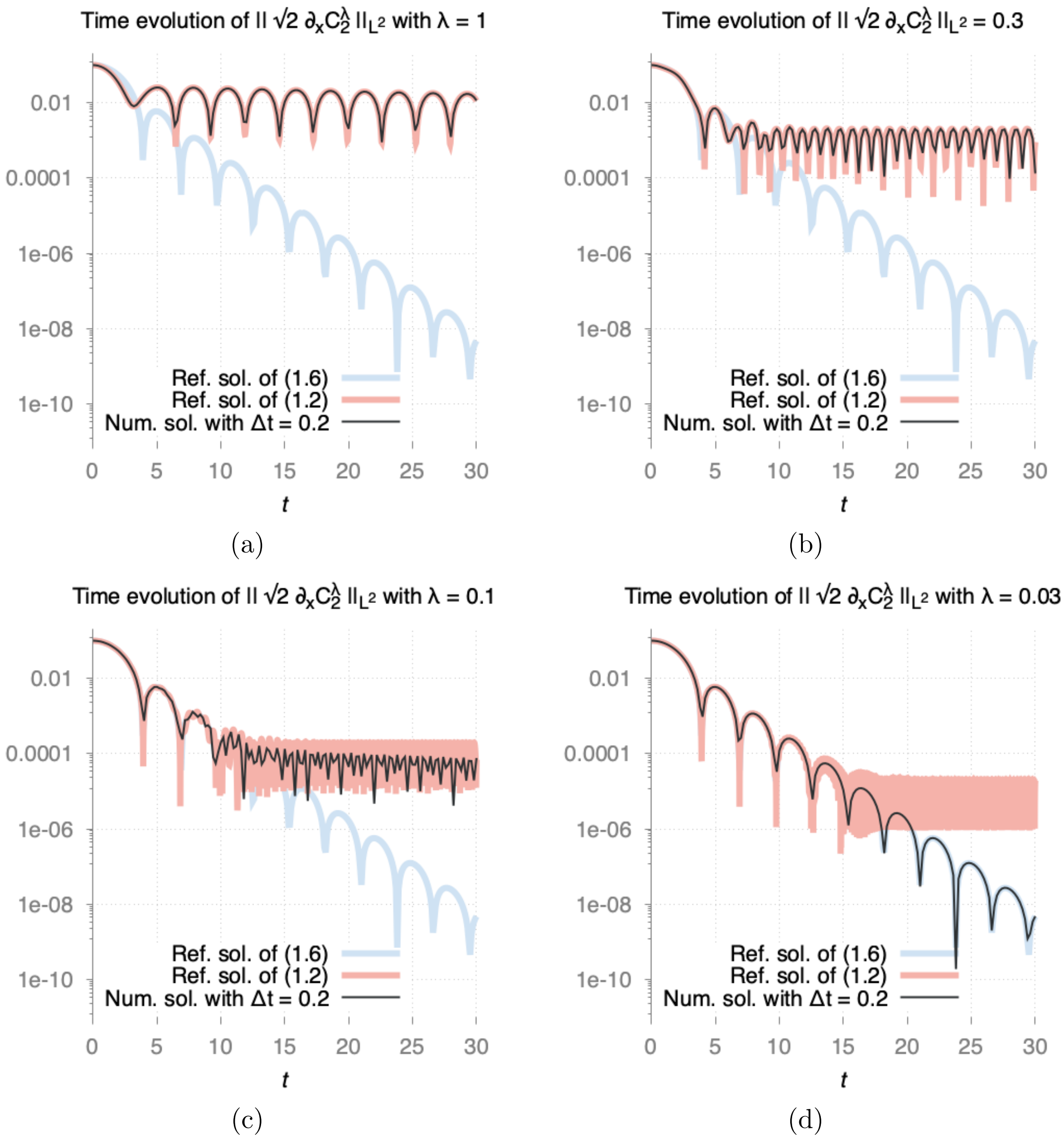

FIGURE 4.6. **Smooth perturbation of equilibrium test case:** time evolution of $\|\sqrt{2}\partial_x C_2^\lambda\|_{L^2}$ in logarithmic scale with *(a)* $\lambda = 1$; *(b)* $\lambda = 3.\,10^{-1}$; *(c)* $\lambda = 10^{-1}$ and *(d)* $\lambda = 3.10^{-2}$.

this case, a large number of Hermite modes is required to adequately describe oscillations in velocity. The numerical results are reported in Figures 4.8 and 4.9 and compared with the reference solution. For $\lambda = 1$ and 10^{-1}, the coarse mesh allows to describe precisely the time oscillations (Figures 4.8 and 4.9 (a)-(b)). When λ becomes smaller, the time step $\Delta t = 0.1$ is too large to provide an approximation of the fast scales, but the slow scale, corresponding to the quasineutral asymptotic model, is still well approximated (see Figures 4.8-(c) and (d) and 4.9-(c) and (d)). Finally, in Figure 4.10, we present several time snapshots of the perturbation $f^\lambda - \mathcal{M}$, where $\mathcal{M}$ is the homogeneous Maxwellian equilibrium with $\lambda = 10^{-3}$. When $t = 25$, we observe the oscillation of f^λ around the equilibrium corresponding to the "echo" of the electric field previously discussed.

4.4. **Two-stream instability.** In this last example, we consider the two stream instability problem with initial distribution

$$f_{\rm in}(x,v) = \frac{1}{6\sqrt{2\pi\, T_{\rm in}(x)}}\left(1+\frac{5\,|v|^2}{T_{\rm in}(x)}\right)\exp\left(-\frac{|v|^2}{2T_{\rm in}(x)}\right), \tag{4.5}$$

and with $T_{\rm in}$ given by

$$T_{\rm in}(x) = 1 + \delta\,\cos(k_x x)\,.$$

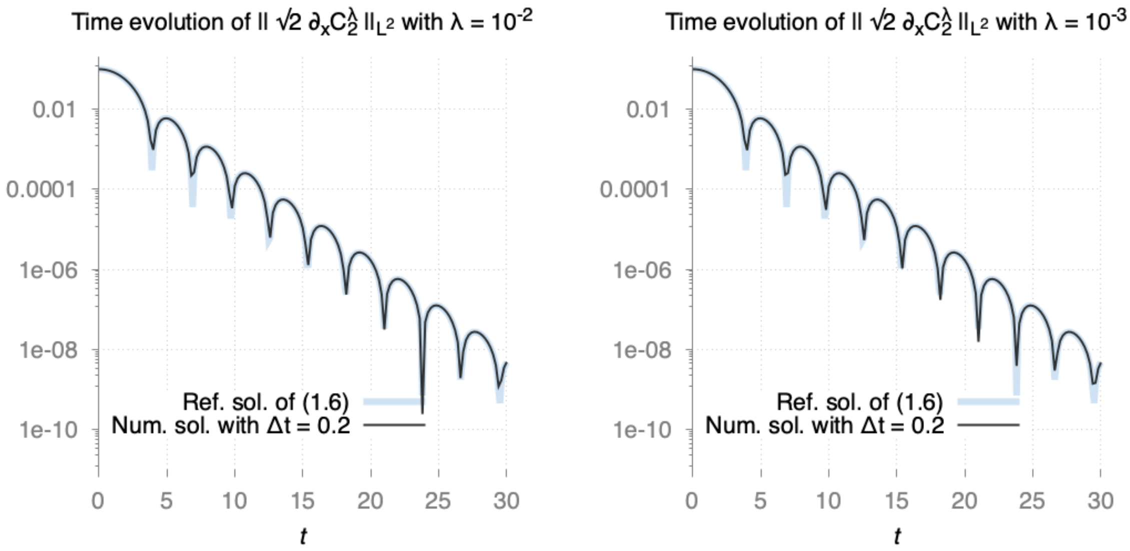

(a) (b)

FIGURE 4.7. **Smooth perturbation of equilibrium test case:** time evolution of $\|\sqrt{2}\partial_x C_2^\lambda\|_{L^2}$ in logarithmic scale with (a) $\lambda = 10^{-2}$ and (b) $\lambda = 3.\ 10^{-3}$.

The other parameters are $\delta = 0.01$, $x \in [-6, 6]$ and $k_x = \pi/6$. The reference solution is obtained with the second order scheme of Section 3.4 on a fine mesh with $N_H = 2000$, $N_x = 2000$ and $\Delta t = 10^{-4}$. This permits, as before, to observe both fast and slow scales of the solution for different values of λ. The time evolution of the L^2 norm of the electric field E^λ and of the slow component $E^\lambda_{\text{slow}} = \sqrt{2}\partial_x C_2^\lambda$ are again computed and shown in Figure 4.11 for different values of λ. The dynamics is such that an instability is firstly developed and then stabilizes due to nonlinear effects. We observe that the norm of E^λ on the time interval $[0, 6]$ strongly oscillates with a frequency inversely proportional to λ and grows exponentially with a rate independent of λ. For larger times, the instability rate increases as λ decreases. The evolution of E^λ_{slow} follows a similar growth dynamics, without exhibiting an oscillatory behavior. In the situation depicted, the rise of the instability is due to the slow part of the electric field and so to the slow part of the dynamics, meaning that the limiting system is not globally well-posed. Figure 4.12 presents the evolution of the same quantities as of Figure 4.11 with a scale of t/λ. This permits to understand that the instability is of the order of $O(e^{\kappa t/\lambda})$. Finally, in Figure 4.13, the distribution function f^λ for $\lambda = 0.02$ at different times is shown. At time $t = 8$, we observe several vortices in the phase space (x, v), this well illustrates the complexity of the dynamics presented when λ is small. To conclude, the results show that, for the initial data considered, the quasineutral limit is not valid for large times. This is also consistent with the theoretical results presented in [27].

5. Conclusion and perspectives

In this work, we proposed a new numerical scheme for the Vlasov-Poisson system able to overcome the strong restrictions due to the fast scale dynamics related to quasineutrality in plasmas. This discretization is quite different from those previously proposed in the literature, as it does not seek to reformulate the Poisson equation into an equivalent wave-type equation. Instead, it discretizes the Poisson equation simultaneously with the equations governing the time evolution of the moments of the Vlasov equation. Our approach expands the distribution function in velocity space using Hermite functions, this enables to study the quasineutral limit by explicitly separating the oscillatory part from the rest of the solution and permits to obtain error estimates both at the continuous as well as the discrete level. A time-splitting method, where the first step involves solving the linearized system around the Maxwellian stationary state and the second step solves the non linear component of the solution completes the scheme.

In a second part, we have proposed several numerical simulations for stable and unstable initial conditions. We have recovered the theoretical convergence order estimates for well-prepared initial data. In these situations and when the time step is very large compared to λ, the numerical scheme filters out the rapid oscillations and captures the asymptotic limit. Moreover, our numerical simulations indicate that when the quasineutral limit, in the long time behavior, is not valid anymore, the scheme loses stability.We

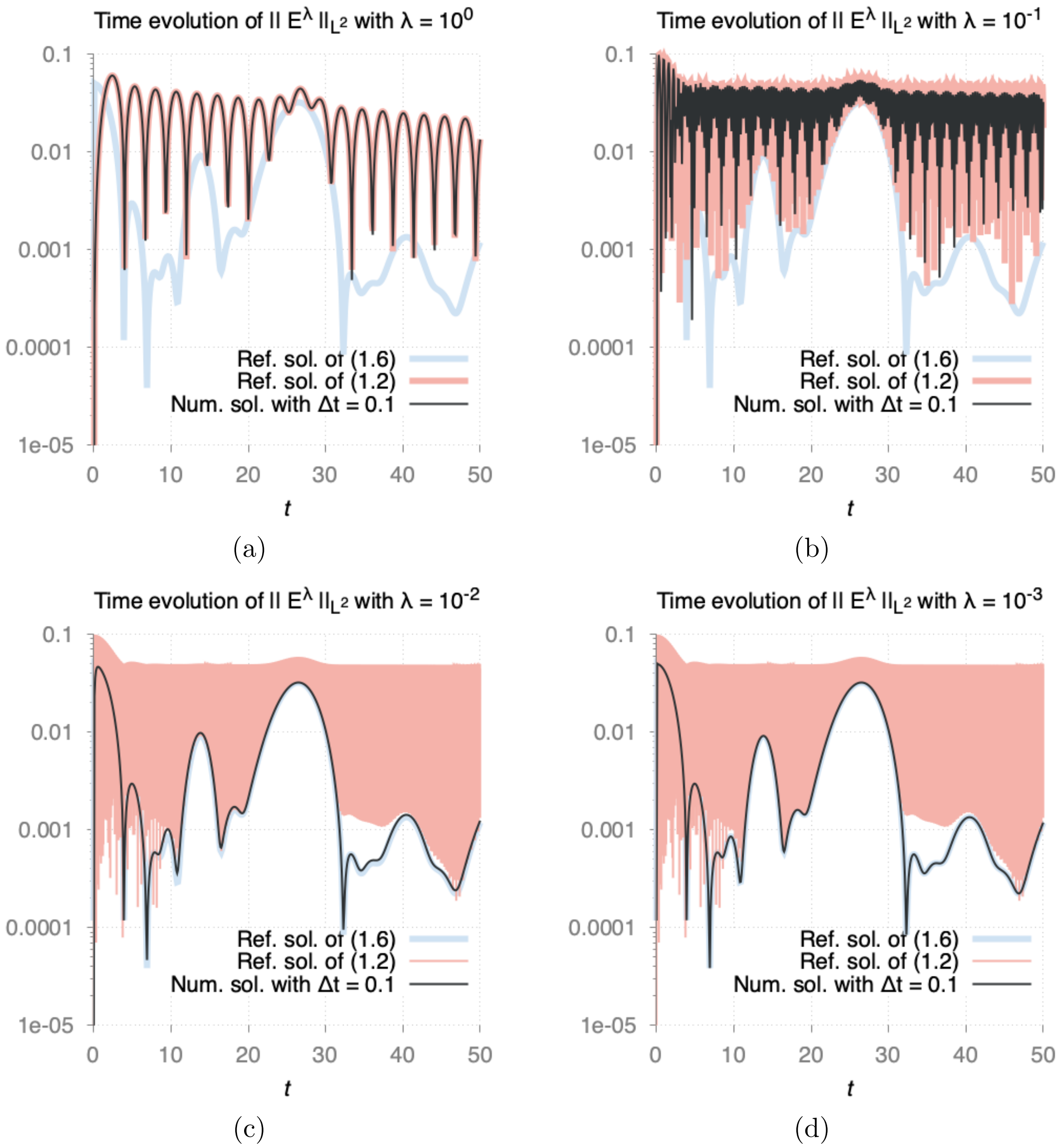

Figure 4.8. **Oscillatory perturbation from equilibrium test case:** time evolution of $\|E^\lambda\|_{L^2}$ in logarithmic scale with (*a*) $\lambda = 1$; (*b*) $\lambda = 10^{-1}$; (*c*) $\lambda = 10^{-2}$ and (*d*) $\lambda = 10^{-3}$.

stress that this lack of uniform stability should not be considered as a limit of the scheme but rather of the model.

While understanding the quasineutral limit remains an open problem within the framework of kinetic theory, a wealth of perspectives emerge, both from the theoretical and numerical viewpoints from the presented results. Starting from the error estimates of the electric field error obtained, it appears feasible to obtain a strong convergence result provided that the rapid oscillations in the electric field are filtered out. Concerning the analysis of the numerical scheme, it appears crucial to gain a better understanding of the stability of the scheme with respect to the discretization parameters and the Debye length. Furthermore, extending the proposed method to the multi-dimensional case represents an important step for realistic applications.

Acknowledgement

The authors are partially funded by the ANR Project Muffin (ANR-19-CE46-0004).

The authors acknowledge the support of the CDP C2EMPI, as well as the French State under the France-2030 programme, the University of Lille, the Initiative of Excellence of the University of Lille, the European Metropolis of Lille for their funding and support of the R-CDP-24-004-C2EMPI project.

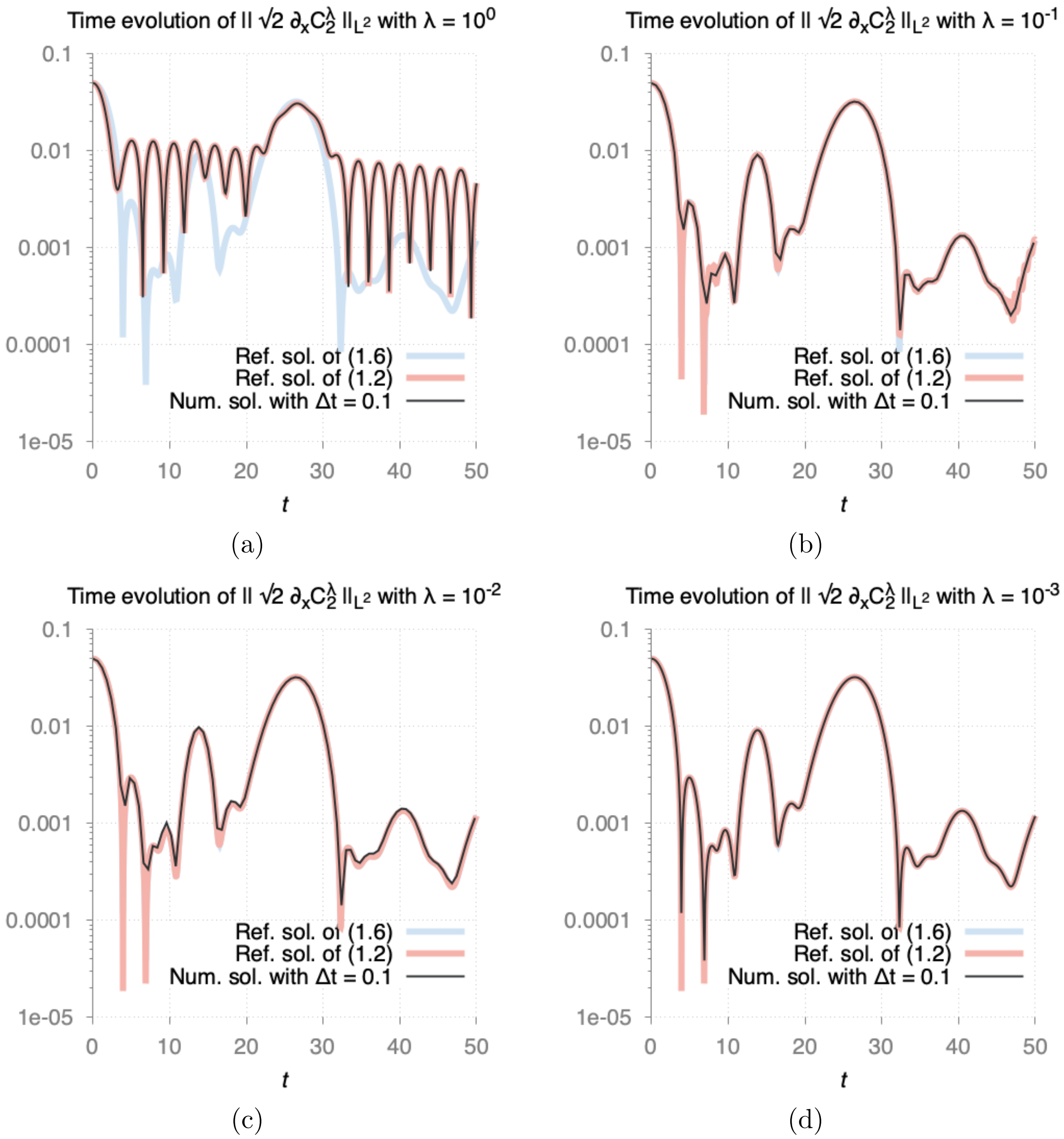

FIGURE 4.9. **Oscillatory perturbation from equilibrium test case:** time evolution of $\|\sqrt{2}\partial_x C_2^\lambda\|_{L^2}$ in logarithmic value with *(a)* $\lambda = 1$; *(b)* $\lambda = 10^{-1}$; *(c)* $\lambda = 10^{-2}$ and *(d)* $\lambda = 10^{-3}$.

APPENDIX A. PROOF OF PROPOSITION 2.1

We fix some time $t \in [0, T]$ and prove that the right hand side in the Duhamel formula (2.10) is of order $\lambda^{1-\alpha}$. To this aim, we distinguish linear and nonlinear terms in $\mathbf{S}^\lambda$. Then, to identify the nonlinear terms and their scaling in λ, we replace $\partial_t C_2^\lambda$ according to (2.5) with $k = 2$ and C_0^λ according to the second line of (2.5) in $\mathbf{S}^\lambda$, we obtain

$$\mathbf{U}^\lambda(t) \;=\; -\int_0^t \exp\left(\frac{s-t}{\lambda}J\right)(\mathbf{N}^\lambda + \mathbf{L}^\lambda)(s)\,\mathrm{d}s\,, \tag{A.1}$$

where $\mathbf{N}^\lambda$ and $\mathbf{L}^\lambda$ are given as follows

$$\mathbf{N}^\lambda \;=\; 2\,T_0^{1/2}\partial_x\begin{pmatrix} C_1^\lambda E^\lambda \\ 0\end{pmatrix} - \frac{\lambda}{2}\,\partial_x\begin{pmatrix} 0 \\ |E^\lambda|^2\end{pmatrix}; \qquad \mathbf{L}^\lambda \;=\; -\,T_0^{3/2}\partial_x^2\begin{pmatrix}\sqrt{6}\,C_3^\lambda + 2\,C_1^\lambda \\ 0\end{pmatrix} + \lambda\,T_0\,\partial_x^2\begin{pmatrix} 0 \\ E^\lambda\end{pmatrix}.$$

To control the contribution of $\mathbf{L}^\lambda$, we apply a standard Laplace method for oscillating integrals and use assumptions (2.11)-(2.12) to control the time derivatives of C_1^λ and C_3^λ. The nonlinear contribution $\mathbf{N}^\lambda$ is more intricate since $|E^\lambda|^2$ may behave like $O(\lambda^{-2\alpha})$. However, we show that the singular terms are solely due to fast oscillations, which are small as $\lambda \to 0$.

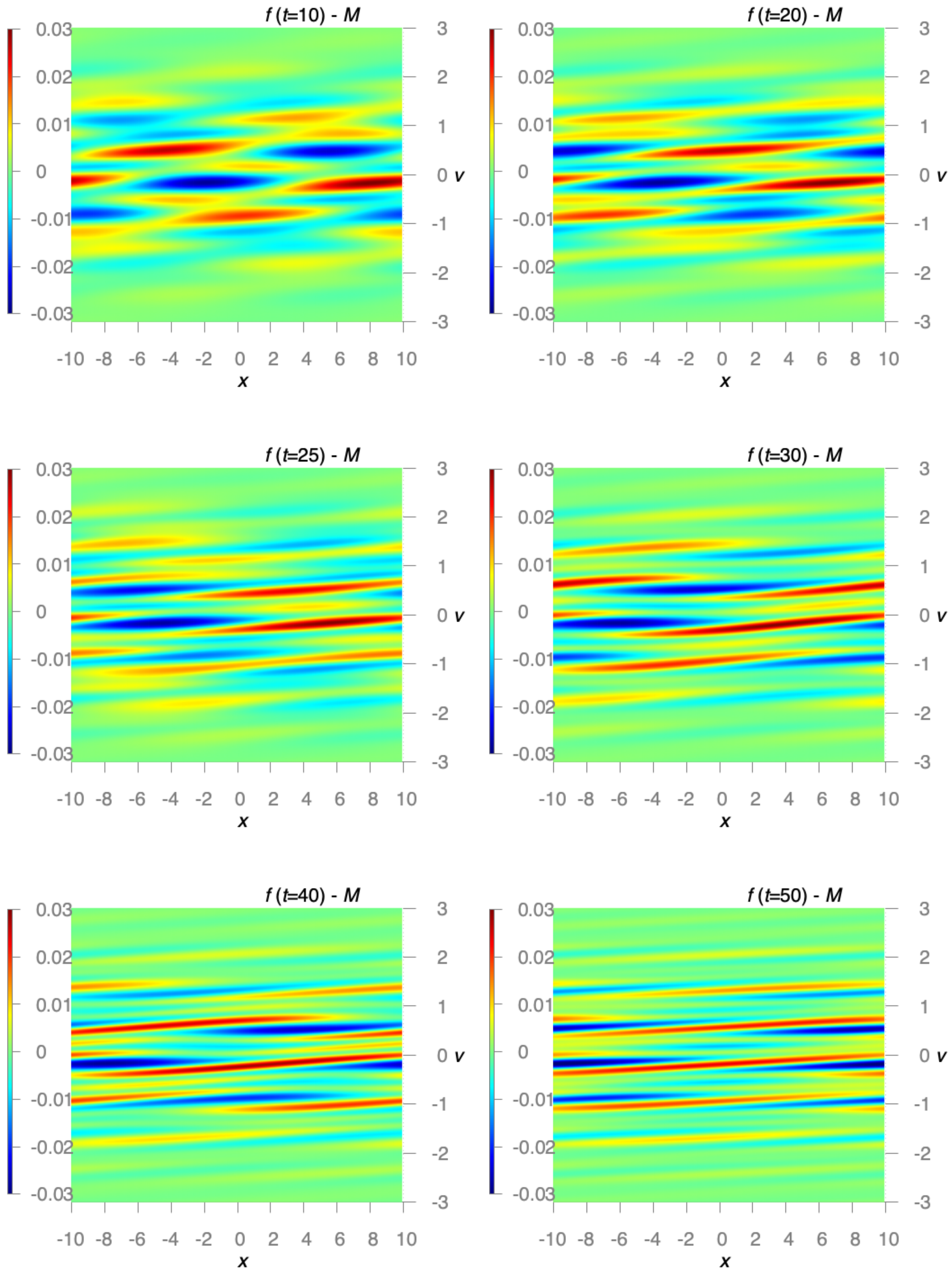

FIGURE 4.10. **Oscillatory perturbation from equilibrium test case:** snapshots of the distribution function $f^\lambda - \mathcal{M}$ at time $t = 10$; 20 ; 25 ; 30 ; 40 and 50 for $\lambda = 10^{-3}$.

First, we replace C_1^λ in $\mathbf{N}^\lambda$ according to the Ampère equation (2.7), which yields

$$\mathbf{N}^\lambda(s) \;=\; -\,\lambda^2\,\partial_s\partial_x \begin{pmatrix} |E^\lambda(s)|^2 \\ 0 \end{pmatrix} \;-\; \frac{\lambda}{2}\,\partial_x \begin{pmatrix} 0 \\ |E^\lambda(s)|^2 \end{pmatrix}\,,$$

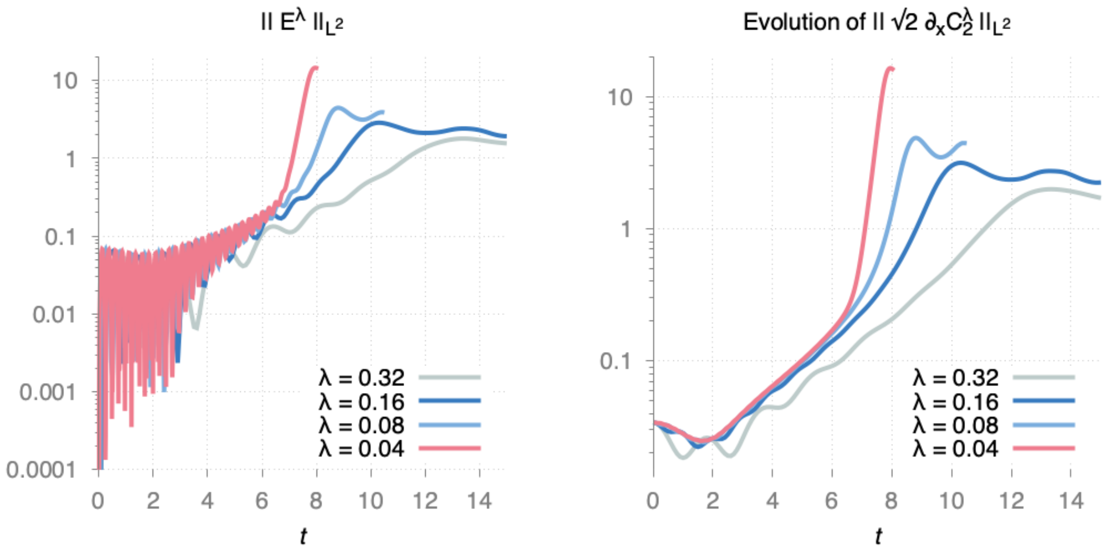

(a) (b)

FIGURE 4.11. **Two-stream instability test case :** time evolution of (a) $\|E^\lambda\|_{L^2}$ and (b) $\|\sqrt{2}\partial_x C_2^\lambda\|_{L^2}$ in logarithmic scale.

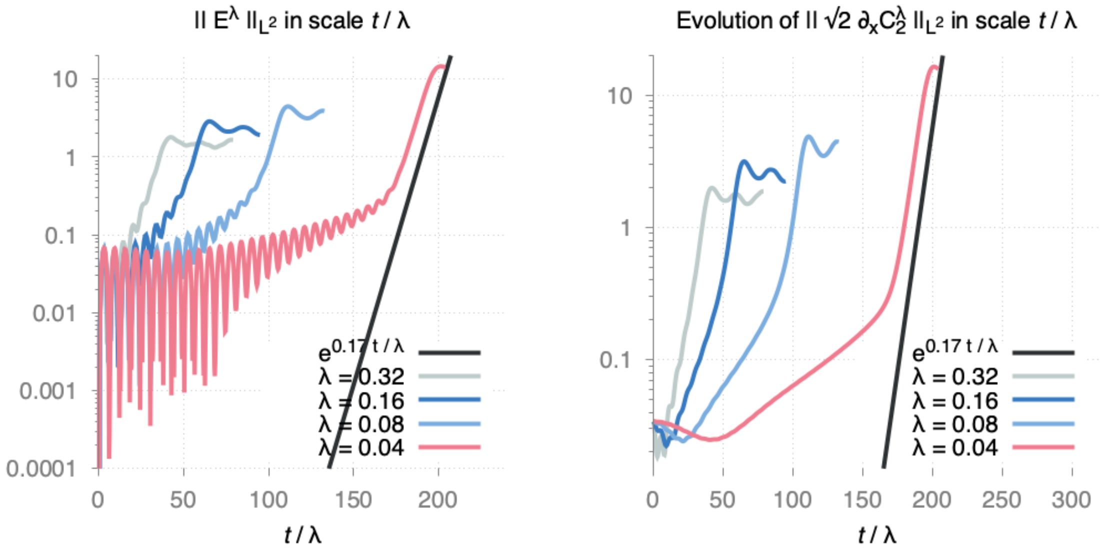

(a) (b)

FIGURE 4.12. **Two-stream instability test casr:** evolution of (a) $\|E^\lambda\|_{L^2}$ and (b) $\|\sqrt{2}\partial_x C_2^\lambda\|_{L^2}$ in logarithmic scale with respect to t/λ.

where we also applied the relation $2E^\lambda\partial_s E^\lambda = \partial_s|E^\lambda|^2$. Multiplying the latter formula by $\exp(sJ/\lambda)$, applying Leibniz rule for products and using the definition of J below (1.11), yields

$$\exp\left(\frac{s}{\lambda}J\right)\cdot \mathbf{N}^\lambda(s) = -\lambda^2\,\partial_s\left(\exp\left(\frac{s}{\lambda}J\right)\cdot\partial_x\begin{pmatrix}|E^\lambda(s)|^2\\ 0\end{pmatrix}\right) - \frac{3\lambda}{2}\exp\left(\frac{s}{\lambda}J\right)\cdot\partial_x\begin{pmatrix}0\\ |E^\lambda(s)|^2\end{pmatrix}. \tag{A.2}$$

The main difficulty comes from the second term in the latter right hand side, which we estimate computing explicitly the contribution of the singular terms in the expansion of E^λ as $\lambda \to 0$. More precisely, we substitute E^λ thanks to the relation

$$E^\lambda = \mathbf{U}_1^\lambda + E^\lambda_{\text{slow}} + E^\lambda_{\text{osc}}\,,$$

where $\mathbf{U}_1^\lambda$ denotes the first component of $\mathbf{U}^\lambda$ and where E^λ_{osc}, given by (2.14), contains the singular terms in the expansion of E^λ. Hence, we have

$$\frac{1}{2}\,\partial_x|E^\lambda|^2 = \mathbf{U}_1^\lambda\,\partial_x E^\lambda + E^\lambda_{\text{osc}}\,\partial_x\mathbf{U}_1^\lambda + \frac{1}{2}\partial_x|E^\lambda_{\text{osc}}|^2 + E^\lambda_{\text{osc}}\,\partial_x E^\lambda_{\text{slow}} + E^\lambda_{\text{slow}}\,\partial_x E^\lambda\,,$$

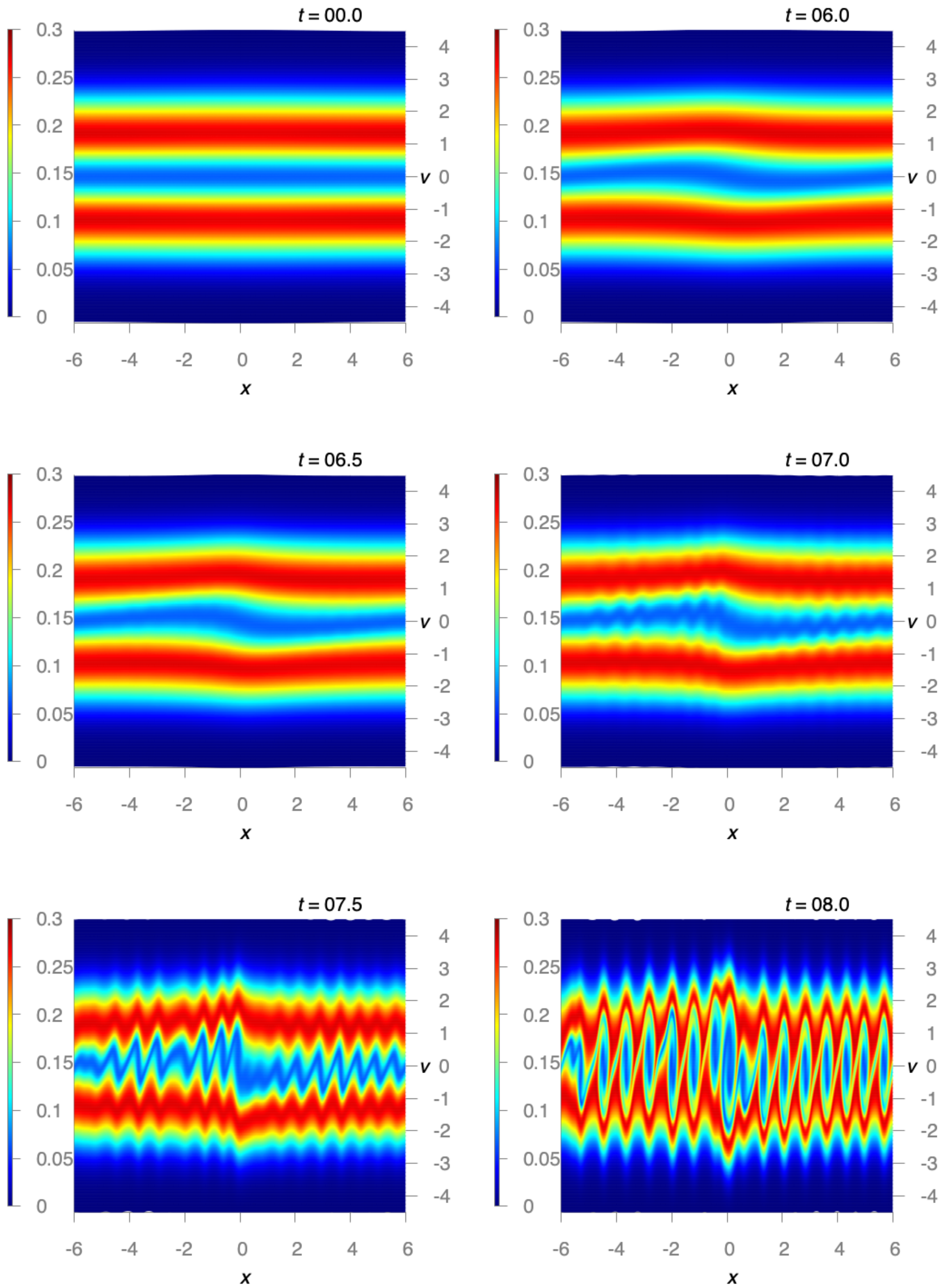

FIGURE 4.13. **Two-stream instability test case:** snapshots of the distribution function f^λ at time $t = 0$; 6 ; 6.5 ; 7 ; 7.5 and 8 for $\lambda = 0.04$.

We replace $|E^\lambda|^2$ according to the latter relation in the second term on the right hand side of (A.2) and obtain

(A.3) $$\exp\left(\frac{s}{\lambda}J\right)\cdot \mathbf{N}^\lambda \;=\; -\lambda^2\,\partial_s\left(\exp\left(\frac{s}{\lambda}J\right)\cdot \mathbf{N}_1^\lambda\right) \;-\; \exp\left(\frac{s}{\lambda}J\right)\cdot\left(A_1\,\mathbf{U}_1^\lambda + A_2\,\partial_x \mathbf{U}_1^\lambda + \;\lambda\,\mathbf{N}_2^\lambda\right),$$

where $(\mathbf{N}_1^\lambda, \mathbf{N}_2^\lambda)$ and (A_1, A_2) are given as follows

$$\mathbf{N}_1^\lambda(s) \,=\, \partial_x \begin{pmatrix} |E^\lambda(s)|^2 \\ 0 \end{pmatrix}; \qquad A_1(s) \,=\, 3\,\lambda \begin{pmatrix} 0 \\ \partial_x E^\lambda(s) \end{pmatrix}; \qquad A_2(s) \,=\, 3\,\lambda \begin{pmatrix} 0 \\ E^\lambda_{\mathrm{osc}}(s) \end{pmatrix};$$

whereas

$$\mathbf{N}_2^\lambda(s) \,=\, 3 \begin{pmatrix} 0 \\ \frac{1}{2}\partial_x |E^\lambda_{\mathrm{osc}}(s)|^2 + E^\lambda_{\mathrm{osc}}(s)\,\partial_x E^\lambda_{\mathrm{slow}}(s) + E^\lambda_{\mathrm{slow}}(s)\partial_x E^\lambda(s) \end{pmatrix}(s)\,.$$

Then, we substitute $\mathbf{N}^\lambda$ in (A.1) according to (A.3) and obtain

$$\mathbf{U}^\lambda(t) = \int_0^t \exp\left(\frac{s-t}{\lambda} J\right) \cdot \Big(A_1(s)\mathbf{U}_1^\lambda(s) + A_2(s)\partial_x \mathbf{U}_1^\lambda(s)\Big)\,\mathrm{d}s + B(t)\,, \tag{A.4}$$

where A_1 and A_2 are given below (A.3) and B gathers all the other terms, that is

$$B(t) = \int_0^t \exp\left(\frac{s-t}{\lambda} J\right) \cdot (\lambda\,\mathbf{N}_2^\lambda(s) - \mathbf{L}^\lambda(s))\,\mathrm{d}s + \lambda^2\,\mathbf{N}_1^\lambda(t) - \lambda^2 \exp\left(-\frac{t}{\lambda}J\right)\cdot \mathbf{N}_1^\lambda(0)\,,$$

where $\mathbf{L}^\lambda$ is given in (A.1) whereas $\mathbf{N}_1^\lambda$, $\mathbf{N}_2^\lambda$ are given in (A.3).

Our strategy is to prove that A_1, A_2 and B are of order $O(\lambda^{1-\alpha})$ and iterate the Duhamel formula (A.4) to gain powers of λ.

<u>Step 1.</u> Upper bound of A_1, A_2 and B. Let us estimate A_1, A_2 and B, given in (A.4), starting with B, which contains the main difficulty, due to the contribution of $\mathbf{N}_2^\lambda$. To estimate B, we reformulate the first term of $\mathbf{L}^\lambda$, defined in (A.1), which is given by

$$\mathbf{L}_1^\lambda \,=\, -\,T_0^{3/2}\partial_x^2 \begin{pmatrix} \sqrt{6}\,C_3^\lambda + 2\,C_1^\lambda \\ 0 \end{pmatrix}.$$

We multiply $\mathbf{L}_1^\lambda$ by $\exp(sJ/\lambda)$ and apply Leibniz rule for products, which yields

$$\exp\left(\frac{s}{\lambda}J\right)\cdot \mathbf{L}_1^\lambda \,=\, \lambda\,J^{-1}\,\partial_s\left(\exp\left(\frac{s}{\lambda}J\right)\cdot \mathbf{L}_1^\lambda\right) - \lambda\,J^{-1}\exp\left(\frac{s}{\lambda}J\right)\cdot \partial_t\,\mathbf{L}_1^\lambda\,.$$

Next, since $J^{-1} = -J$ and since J and $\exp\left(\frac{s}{\lambda}J\right)$ commute, we obtain

$$\exp\left(\frac{s}{\lambda}J\right)\cdot \mathbf{L}_1^\lambda \,=\, -\,\lambda\,\partial_s\left(\exp\left(\frac{s}{\lambda}J\right)\cdot T_0^{3/2}\partial_x^2\begin{pmatrix} 0 \\ \sqrt{6}\,C_3^\lambda + 2\,C_1^\lambda \end{pmatrix}\right) + \lambda\exp\left(\frac{s}{\lambda}J\right)\cdot T_0^{3/2}\partial_t\partial_x^2\begin{pmatrix} 0 \\ \sqrt{6}\,C_3^\lambda + 2\,C_1^\lambda \end{pmatrix}.$$

According to the latter relation, the product between $\exp(sJ/\lambda)$ and $\mathbf{L}^\lambda$ satisfies

$$\exp\left(\frac{s}{\lambda}J\right)\cdot \mathbf{L}^\lambda \,=\, -\lambda\,\partial_s\left(\exp\left(\frac{s}{\lambda}J\right)\cdot \mathbf{L}_2^\lambda\right) \,+\, \lambda\exp\left(\frac{s}{\lambda}J\right)\cdot \mathbf{L}_3^\lambda\,, \tag{A.5}$$

where $\mathbf{L}_2^\lambda$ and $\mathbf{L}_3^\lambda$ are given as follows

$$\mathbf{L}_2^\lambda \,=\, T_0^{3/2}\partial_x^2\begin{pmatrix} 0 \\ \sqrt{6}\,C_3^\lambda + 2\,C_1^\lambda \end{pmatrix}; \qquad \mathbf{L}_3^\lambda \,=\, T_0^{3/2}\partial_s\partial_x^2\begin{pmatrix} 0 \\ \sqrt{6}\,C_3^\lambda + 2\,C_1^\lambda \end{pmatrix} \,+\, T_0\begin{pmatrix} 0 \\ \partial_x^2 E^\lambda \end{pmatrix}.$$

We replace $\mathbf{L}^\lambda$ according to (A.5) in the definition of B in (A.4), we find

$$B(t) = \lambda\int_0^t \exp\left(\frac{s-t}{\lambda}J\right)\cdot(\mathbf{N}_2^\lambda - \mathbf{L}_3^\lambda)(s)\,\mathrm{d}s \,+\, \lambda\,(\lambda\,\mathbf{N}_1^\lambda + \mathbf{L}_2^\lambda)(t) \,-\, \lambda\exp\left(-\frac{t}{\lambda}J\right)\cdot(\lambda\,\mathbf{N}_1^\lambda + \mathbf{L}_2^\lambda)(0)\,.$$

We take the L^2 norm of the l-th derivative and apply the triangle inequality in the latter relation

$$\begin{aligned} \left\|\partial_x^l B(t)\right\|_{L^2} \le \lambda\left\|\partial_x^l\int_0^t \exp\left(\frac{s}{\lambda}J\right)\cdot \mathbf{N}_2^\lambda(s)\,\mathrm{d}s\right\|_{L^2} + \lambda\left\|\partial_x^l\int_0^t \exp\left(\frac{s}{\lambda}J\right)\cdot \mathbf{L}_3^\lambda(s)\,\mathrm{d}s\right\|_{L^2} \\ + \lambda^2\left\|\partial_x^l \mathbf{N}_1^\lambda(t)\right\|_{L^2} + \lambda\left\|\partial_x^l \mathbf{L}_2^\lambda(t)\right\|_{L^2} + \lambda^2\left\|\partial_x^l \mathbf{N}_1^\lambda(0)\right\|_{L^2} + \lambda\left\|\partial_x^l \mathbf{L}_2^\lambda(0)\right\|_{L^2}. \end{aligned} \tag{A.6}$$

To estimate the first term in the right hand side of (A.6), we substitute $\mathbf{N}_2^\lambda$ according to its definition below (A.3) and apply the triangle inequality, which yields

$$\lambda \left\| \partial_x^l \int_0^t \exp\left(\frac{s}{\lambda} J\right) \cdot \mathbf{N}_2^\lambda \mathrm{d}s \right\|_{L^2} \leq \mathcal{N}_{21}(t) + \mathcal{N}_{22}(t) \,,$$

where

$$\begin{cases} \mathcal{N}_{21}(t) \,=\, \dfrac{3\lambda}{2} \left\| \partial_x^l \displaystyle\int_0^t \exp\left(\frac{s}{\lambda} J\right) \cdot \partial_x \begin{pmatrix} 0 \\ |E_{\text{osc}}^\lambda|^2 \end{pmatrix} \mathrm{d}s \right\|_{L^2} \,, \\ \mathcal{N}_{22}(t) \,=\, 3\lambda \left\| \partial_x^l \displaystyle\int_0^t \exp\left(\frac{s}{\lambda} J\right) \cdot \begin{pmatrix} 0 \\ E_{\text{osc}}^\lambda \sqrt{2}\, T_0\, \partial_x^2 C_2^\lambda + \sqrt{2}\, T_0\, \partial_x C_2^\lambda \partial_x E^\lambda \end{pmatrix} \mathrm{d}s \right\|_{L^2} . \end{cases}$$

The estimate for $\mathcal{N}_{21}(t)$ is most intricate since E_{osc}^λ, given by (2.14), is of order $O(\lambda^{-\alpha})$. We compute the time integral in $\mathcal{N}_{21}(t)$ explicitly and show that the singularity cancels due to the fast oscillations of E_{osc}^λ. To make computations more tractable, we identify $\exp(sJ/\lambda)$ and E_{osc}^λ in $\mathcal{N}_{21}(t)$ with their complex representation

$$\exp\left(\frac{s}{\lambda} J\right) \,=\, e^{-i\frac{s}{\lambda}} \quad ; \quad \begin{pmatrix} 0 \\ |E_{\text{osc}}^\lambda|^2 \end{pmatrix} \,=\, i \left| E_{\text{osc}}^\lambda \right|^2 \quad ; \quad E_{\text{osc}}^\lambda(s) \,=\, \frac{z e^{i\frac{s}{\lambda}} + \bar{z} e^{-i\frac{s}{\lambda}}}{2} \,,$$

where the time independent complex number z is given by $z = \left(E^\lambda - \sqrt{2}\, T_0\, \partial_x C_2^\lambda\right)(0) + i\sqrt{T_0} C_1^\lambda(0)/\lambda$. We reformulate $\mathcal{N}_{21}(t)$ according to the latter relations

$$\mathcal{N}_{21}(t) \,=\, \frac{3\lambda}{2} \left\| \partial_x^{l+1} \int_0^t e^{-i\frac{s}{\lambda}}\, i \left| \frac{z e^{i\frac{s}{\lambda}} + \bar{z} e^{-i\frac{s}{\lambda}}}{2} \right|^2 \mathrm{d}s \right\|_{L^2} .$$

We expand the square in the latter expression and compute the time integral explicitly:

$$\mathcal{N}_{21}(t) \,=\, \frac{3\lambda^2}{2} \left\| \partial_x^{l+1} \left(\frac{|z|^2}{2} \left(1 - e^{-i\frac{t}{\lambda}}\right) + \frac{z^2}{4} \left(e^{i\frac{t}{\lambda}} - 1\right) + \frac{\bar{z}^2}{12} \left(1 - e^{-3i\frac{t}{\lambda}}\right) \right) \right\|_{L^2} .$$

Then, we apply Leibniz rule to develop the derivatives in x of order $l+1$ and estimate each product thanks to Cauchy-Schwarz inequality, which yields

$$\mathcal{N}_{21}(t) \,\leq\, C\, \lambda^2\, \|z\|^2_{W^{l+1,4}} \,,$$

for some constant C depending on $l \geq 0$. We replace z according to $z = \left(E^\lambda - \sqrt{2}\, T_0\, \partial_x C_2^\lambda\right)(0) - i\sqrt{T_0} C_1^\lambda(0)/\lambda$ and apply the triangle inequality in the latter relation and obtain

$$\mathcal{N}_{21}(t) \,\leq\, C \left(\lambda^2 \left\| C_2^\lambda(0) \right\|^2_{W^{l+2,4}} + \lambda^2 \left\| E^\lambda(0) \right\|^2_{W^{l+1,4}} + \left\| C_1^\lambda(0) \right\|^2_{W^{l+1,4}} \right) .$$

To estimate $\mathcal{N}_{22}(t)$, we bound the time integral thanks to Jensen inequality and then take the supremum in time, this yields

$$\mathcal{N}_{22}(t) \,\leq\, 3\,\lambda\, t \sup_{0\leq s\leq T} \left(\left\| \partial_x^l \left(E_{\text{osc}}^\lambda(s) \sqrt{2}\, T_0\, \partial_x^2 C_2^\lambda(s) \right) \right\|_{L^2} + \left\| \partial_x^l \left(\sqrt{2}\, T_0\, \partial_x C_2^\lambda(s) \partial_x E^\lambda(s) \right) \right\|_{L^2} \right) .$$

Then, we apply Leibniz rule to develop the derivatives of order l and estimate each product thanks to Cauchy-Schwarz inequality, which yields

$$\mathcal{N}_{22}(t) \,\leq\, C\,\lambda \sup_{0\leq s\leq T} \left(\left\| C_2^\lambda(s) \right\|_{W^{l+2,4}} \left\| E_{\text{osc}}^\lambda(s) \right\|_{W^{l,4}} + \left\| C_2^\lambda(s) \right\|_{W^{l+1,4}} \left\| E^\lambda(s) \right\|_{W^{l+1,4}} \right) ,$$

for some constant C depending on $l \geq 0$, on the final time T and the temperature T_0. We estimate E_{osc}^λ with the triangular inequality, which yields

$$\mathcal{N}_{22}(t) \,\leq\, C\,\lambda \sup_{0\leq s\leq T} \left(\left\| C_2^\lambda(s) \right\|_{W^{l+2,4}} \left(\|E^\lambda(0)\|_{W^{l,4}} + \|C_2^\lambda(0)\|_{W^{l+1,4}} + \lambda^{-1} \|C_1^\lambda(0)\|_{W^{l,4}} + \|E^\lambda(s)\|_{W^{l+1,4}} \right) \right) ,$$

and then apply Young inequality to estimate each product, which yields

$$\mathcal{N}_{22}(t) \,\leq\, C \sup_{0\leq s\leq T} \left(\lambda^{1-\alpha} \left\| C_2^\lambda(s) \right\|^2_{W^{l+2,4}} + \lambda^{\alpha-1} \left\| C_1^\lambda(0) \right\|^2_{W^{l,4}} + \lambda^{1+\alpha} \left\| E^\lambda(s) \right\|^2_{W^{l+1,4}} \right) ,$$

for all $0<\lambda<1$. Gathering our estimates on $\mathcal{N}_{21}$ and $\mathcal{N}_{22}$, we obtain

$$\begin{aligned}\lambda \left\| \partial_x^l \int_0^t \exp\left(\frac{s}{\lambda} J\right) \cdot \mathbf{N}_2^\lambda \mathrm{d}s \right\|_{L^2} &\leq C \left(\lambda^{\alpha-1} \left\| C_1^\lambda(0) \right\|^2_{W^{l+1,4}} + \lambda^{1+\alpha} \sup_{0\leq s\leq T} \left\| E^\lambda(s) \right\|^2_{W^{l+1,4}} \right) \\ &\quad + C\, \lambda^{1-\alpha} \sup_{0\leq s\leq T} \left\| C_2^\lambda(s) \right\|^2_{W^{l+2,4}} ,\end{aligned} \tag{A.7}$$

for all $0<\lambda<1$ and for some constant C depending on $l\geq 0$, on the final time T and the temperature T_0. We now estimate the second term in the right hand side (A.6) thanks to Jensen inequality

$$\lambda \left\| \partial_x^l \int_0^t \exp\left(\frac{s}{\lambda} J\right) \cdot \mathbf{L}_3^\lambda \mathrm{d}s \right\|_{L^2} \leq \lambda\, t \sup_{0\leq s\leq T} \left\| \partial_x^l \mathbf{L}_3^\lambda(s) \right\|_{L^2} ,$$

where $\mathbf{L}_3^\lambda$ is defined below (A.5). Then, we substitute the time derivatives of C_1^λ and C_3^λ in the expression of $\mathbf{L}_3^\lambda$ thanks to the first line of (2.5) with $k=1$ and $k=3$ respectively, which yields

$$\begin{aligned}&\lambda \left\| \partial_x^l \int_0^t \exp\left(\frac{s}{\lambda} J\right) \cdot \mathbf{L}_3^\lambda \mathrm{d}s \right\|_{L^2} \leq \\ &\lambda T_0 t \sup_{0\leq s\leq T} \left\| \partial_x^{l+2} \left(\sqrt{18}\, E^\lambda C_2^\lambda - \sqrt{18}\, T_0\, \partial_x C_2^\lambda - \sqrt{24}\, T_0\, \partial_x C_4^\lambda + 2 E^\lambda C_0^\lambda - 2T_0\, \partial_x C_0^\lambda \; - \; 2\sqrt{2}\, T_0\, \partial_x C_2^\lambda + E^\lambda \right) \right\|_{L^2} .\end{aligned}$$

We apply the triangle inequality and obtain

$$\begin{aligned}\lambda \left\| \partial_x^l \int_0^t \exp\left(\frac{s}{\lambda} J\right) \cdot \mathbf{L}_3^\lambda \mathrm{d}s \right\|_{L^2} &\leq C\lambda \sup_{0\leq s\leq T} \left(\left\| \partial_x^{l+2} E^\lambda(s) \right\|_{L^2} + \left\| \partial_x^{l+2} (E^\lambda C_2^\lambda)(s) \right\|_{L^2} + \left\| \partial_x^{l+2} (E^\lambda C_0^\lambda)(s) \right\|_{L^2} \right) \\ &\quad + C\lambda \sup_{0\leq s\leq T} \left(\left\| \partial_x^{l+3} C_2^\lambda(s) \right\|_{L^2} + \left\| \partial_x^{l+3} C_4^\lambda(s) \right\|_{L^2} + \left\| \partial_x^{l+3} C_0^\lambda(s) \right\|_{L^2} \right) ,\end{aligned}$$

for some constant C depending on the final time T and the temperature T_0. Then, we apply Leibniz rule to develop the nonlinear terms and estimate each product thanks to Young inequality

$$\begin{aligned}\lambda \left\| \partial_x^l \int_0^t \exp\left(\frac{s}{\lambda} J\right) \cdot \mathbf{L}_3^\lambda \mathrm{d}s \right\|_{L^2} &\leq C \sup_{0\leq s\leq T} \left(\lambda \left\| \partial_x^{l+2} E^\lambda(s) \right\|_{L^2} ,\ \lambda^{1+\alpha} \left\| E^\lambda(s) \right\|^2_{W^{l+2,4}} \right) \\ &\quad + C \sup_{\substack{0\leq s\leq T \\ k=0,2,4}} \left(\lambda \left\| \partial_x^{l+3} C_k^\lambda(s) \right\|_{L^2} ,\ \lambda^{1-\alpha} \left\| C_k^\lambda(s) \right\|^2_{W^{l+2,4}} \right) ,\end{aligned} \tag{A.8}$$

for some constant C depending on $l\geq 0$, on the final time T and the temperature T_0. We use the same method to estimate the last four terms on the right hand side of (A.6) and obtain

$$\begin{aligned}&\lambda^2 \left\| \partial_x^l \mathbf{N}_1^\lambda(t) \right\|_{L^2} + \lambda \left\| \partial_x^l \mathbf{L}_2^\lambda(t) \right\|_{L^2} + \lambda^2 \left\| \partial_x^l \mathbf{N}_1^\lambda(0) \right\|_{L^2} + \lambda \left\| \partial_x^l \mathbf{L}_2^\lambda(0) \right\|_{L^2} \\ &\qquad \leq C\, \lambda^2 \sup_{0\leq s\leq T} \left(\| E^\lambda(s) \|^2_{W^{l+1,4}} \right) + C\, \lambda \sup_{\substack{0\leq s\leq T \\ k=1,3}} \left(\| \partial_x^{l+2} C_k^\lambda(s) \|_{L^2} \right) ,\end{aligned} \tag{A.9}$$

for some constant C depending on $l\geq 0$ and on the temperature T_0. Gathering estimates (A.7), (A.8) and (A.9) in (A.6), we find

$$\begin{aligned}\left\| \partial_x^l B(t) \right\|_{L^2} &\leq C \left(\lambda^{\alpha-1} \left\| C_1^\lambda(0) \right\|^2_{W^{l+1,4}} + \sup_{0\leq s\leq T} \left(\lambda \left\| \partial_x^{l+2} E^\lambda(s) \right\|_{L^2} ,\ \lambda^{1+\alpha} \left\| E^\lambda(s) \right\|^2_{W^{l+2,4}} \right) \right) \\ &\quad + C \sup_{\substack{0\leq s\leq T \\ 0\leq k\leq 4}} \left(\lambda \left\| C_k^\lambda(s) \right\|_{H^{l+3}} ,\ \lambda^{1-\alpha} \left\| C_k^\lambda(s) \right\|^2_{W^{l+2,4}} \right) ,\end{aligned}$$

for all $0<\lambda<1$ and for some constant C depending on $l\geq 0$, on the final time T and the temperature T_0. We sum the latter estimate over all $l\leq n$ and take the supremum in t on the left hand side, which yields

$$\begin{aligned}\sup_{0\leq t\leq T} \| B(t) \|_{H^n} &\leq C \left(\lambda^{\alpha-1} \left\| C_1^\lambda(0) \right\|^2_{W^{n+1,4}} + \sup_{0\leq t\leq T} \left(\lambda \left\| E^\lambda(t) \right\|_{H^{n+2}} ,\ \lambda^{1+\alpha} \left\| E^\lambda(t) \right\|^2_{W^{n+2,4}} \right) \right) \\ &\quad + C \sup_{\substack{0\leq t\leq T \\ 0\leq k\leq 4}} \left(\lambda \left\| C_k^\lambda(t) \right\|_{H^{n+3}} ,\ \lambda^{1-\alpha} \left\| C_k^\lambda(t) \right\|^2_{W^{n+2,4}} \right) ,\end{aligned}$$

for all $0 < \lambda < 1$ and $n \geq 0$, where the constant C depends on $n \geq 0$, on the final time T and the temperature T_0. We bound $L^2(\mathbb{T})$ norms with their $L^4(\mathbb{T})$ counterparts, which yields

$$\sup_{0\le t\le T} \|B(t)\|_{H^n} \le C \left(\lambda^{\alpha-1} \left\| C_1^\lambda(0) \right\|^2_{W^{n+1,4}} + \sup_{0\le t\le T} \left(\lambda \left\| E^\lambda(t) \right\|_{W^{n+2,4}}, \, \lambda^{1+\alpha} \left\| E^\lambda(t) \right\|^2_{W^{n+2,4}} \right) \right)$$
$$+ C \sup_{\substack{0\le t\le T\\ 0\le k\le 4}} \left(\lambda \left\| C_k^\lambda(t) \right\|_{W^{n+3,4}}, \, \lambda^{1-\alpha} \left\| C_k^\lambda(t) \right\|^2_{W^{n+3,4}} \right).$$

To conclude, we fix some $n \in \mathbb{N}^\star$ such that $n \le r_0$ and estimate the norms of E^λ and $C_1^\lambda(0)$ on the first line thanks to assumption (2.11) and the norms of coefficient C_k^λ, $0 \le k \le 4$, on the second line thanks to assumption (2.12). This gives

$$\sup_{0\le t\le T} \|B(t)\|_{H^n} \le \, C\lambda^{1-\alpha}, \tag{A.10}$$

for all $0 < \lambda < 1$ and $0 \le n \le r_0$, where C depends on α, on the final time T, the temperature T_0, the size of the domain $\mathbb{T}$ and the implicit constants in (2.11)-(2.12), and where r_0 is given in (2.11).
Using the same approach, we find the following estimates for A_1 and A_2 (defined by (A.3))

$$\sup_{0\le t\le T} \left(\|A_1(t)\|_{W^{n,\infty}}, \, \|A_2(t)\|_{W^{n,\infty}} \right) \le \, C \sup_{0\le t\le T} \left(\lambda \left\| E^\lambda(t) \right\|_{W^{n+1,\infty}}, \, \left\| C_1^\lambda(0) \right\|_{W^{n,\infty}}, \, \lambda \left\| C_2^\lambda(0) \right\|_{W^{n+1,\infty}} \right).$$

We use Sobolev injections to bound the $L^\infty(\mathbb{T})$ norms with their $W^{1,4}(\mathbb{T})$ counterpart, which yields

$$\sup_{0\le t\le T} \left(\|A_1(t)\|_{W^{n,\infty}}, \, \|A_2(t)\|_{W^{n,\infty}} \right) \le \, C \sup_{0\le t\le T} \left(\lambda \left\| E^\lambda(t) \right\|_{W^{n+2,4}}, \, \left\| C_1^\lambda(0) \right\|_{W^{n+1,4}}, \, \lambda \left\| C_2^\lambda(0) \right\|_{W^{n+2,4}} \right).$$

Using assumption (2.11) to estimate E^λ and C_1^λ and assumption (2.12) for C_2^λ, we find

$$\sup_{0\le t\le T} \left(\|A_1(t)\|_{W^{n,\infty}}, \, \|A_2(t)\|_{W^{n,\infty}} \right) \le \, C\lambda^{1-\alpha}, \tag{A.11}$$

for all $0 < \lambda < 1$ and $0 \le n \le r_0$, where C depends on α, on the final time T, the temperature T_0, the size of the domain $\mathbb{T}$ and the implicit constants in (2.11)-(2.12), and where r_0 is given in (2.11).

Step 2. iteration of the Duhamel formula. We now focus on the iteration process. We consider some integer $l \geq 0$, take the l-th derivative in x and then the $L^2(\mathbb{T})$-norm in (A.4). After applying Jensen inequality to bound the time integral, using that $\exp((s-t)J/\lambda)$ is an isometry of $\mathbb{R}^2$ and using Leibniz rule to estimate the products between A_i , $i \in \{0, 1\}$, and $\mathbf{U}_1^\lambda$, we obtain

$$\sup_{0\le t\le T} \left\| \partial_x^l \mathbf{U}^\lambda(t) \right\|_{L^2} \le \, C \sup_{0\le t\le T} \left(\|A_1(t)\|_{W^{l,\infty}}, \, \|A_2(t)\|_{W^{l,\infty}} \right) \sup_{0\le t\le T} \left\| \mathbf{U}_1^\lambda(t) \right\|_{H^{l+1}} + \sup_{0\le t\le T} \left\| \partial_x^l B(t) \right\|_{L^2},$$

for some constant C depending on $l \geq 0$ and T. We sum the latter estimate over all integers $l \geq 0$ less than n, for any $n \in \mathbb{N}$ such that $n \le r_0$, where r_0 is given in (2.11)

$$\sup_{0\le t\le T} \left\| \mathbf{U}^\lambda(t) \right\|_{H^n} \le \, C \left(\sup_{0\le t\le T} \left(\|A_1(t)\|_{W^{n,\infty}}, \, \|A_2(t)\|_{W^{n,\infty}} \right) \sup_{0\le t\le T} \left\| \mathbf{U}_1^\lambda(t) \right\|_{H^{n+1}} + \sup_{0\le t\le T} \|B(t)\|_{H^n} \right),$$

for some constant C depending on $n \geq 0$ and T. We bound the norms of (A_1, A_2) according to (A.11) and the norm of B according to (A.10), which yields

$$\sup_{0\le t\le T} \left\| \mathbf{U}^\lambda(t) \right\|_{H^n} \le \, C\lambda^{1-\alpha} \left(\sup_{0\le t\le T} \left\| \mathbf{U}_1^\lambda(t) \right\|_{H^{n+1}} + 1 \right),$$

for all $0 < \lambda < 1$ and $0 \le n \le r_0$, where the constant C depends on α, on the final time T, the temperature T_0, the size of the domain $\mathbb{T}$ and the implicit constants in (2.11)-(2.12). Next, we point out that $\left\| \mathbf{U}_1^\lambda \right\|_{H^{n+1}} \le \left\| \mathbf{U}^\lambda \right\|_{H^{n+1}}$, which allows to iterate the latter formula with respect to n and obtain

$$\sup_{0\le t\le T} \left\| \mathbf{U}^\lambda(t) \right\|_{L^2} \le \, C \left(\lambda^{n(1-\alpha)} \sup_{0\le t\le T} \left\| \mathbf{U}_1^\lambda(t) \right\|_{H^{n+1}} + \lambda^{1-\alpha} \right),$$

for all $0 < \lambda < 1$ and $0 \le n \le r_0$. Now, we fix $n = r_0$, and since $r_0 \ge 1/(1-\alpha)$, we obtain

$$\sup_{0\le t\le T} \left\|\mathbf{U}^\lambda(t)\right\|_{L^2} \le C\left(\lambda \sup_{0\le t\le T}\left\|\mathbf{U}_1^\lambda(t)\right\|_{H^{r_0+1}} + \lambda^{1-\alpha}\right),$$

for all $0 < \lambda < 1$, where C depends on α, T, T_0, $\mathbb{T}$ and the implicit constants in (2.11)-(2.12). To bound the norm of $\mathbf{U}_1^\lambda$, we substitute $\mathbf{U}_1^\lambda$ according to the following relation $\mathbf{U}_1^\lambda = E^\lambda - E^\lambda_{\text{slow}} - E^\lambda_{\text{osc}}$ and apply the triangle inequality

$$\sup_{0\le t\le T} \left\|\mathbf{U}^\lambda(t)\right\|_{L^2} \le C\left(\lambda \sup_{0\le t\le T}\left(\left\|E^\lambda(t)\right\|_{H^{r_0+1}} + \left\|C_2^\lambda(t)\right\|_{H^{r_0+2}} + \left\|E^\lambda_{\text{osc}}(t)\right\|_{H^{r_0+1}}\right) + \lambda^{1-\alpha}\right).$$

To bound the norm of E^λ_{osc}, we substitute E^λ_{osc} according to (2.14) and apply the triangle inequality

$$\sup_{0\le t\le T} \left\|\mathbf{U}^\lambda(t)\right\|_{L^2} \le C\left(\sup_{0\le t\le T}\left(\lambda\left\|E^\lambda(t)\right\|_{H^{r_0+1}},\, \left\|C_1^\lambda(0)\right\|_{H^{r_0+1}},\, \lambda\left\|C_2^\lambda(t)\right\|_{H^{r_0+2}}\right) + \lambda^{1-\alpha}\right).$$

We bound E^λ and C_1^λ thanks to (2.11) and C_2^λ thanks to (2.12), which yields the result

$$\sup_{0\le t\le T} \left\|\mathbf{U}^\lambda(t)\right\|_{L^2} \le C\lambda^{1-\alpha},$$

for all $0 < \lambda < 1$ and $0 \le n \le r_0$, where the constant C depends on α, on the final time T, the temperature T_0, the size of the domain $\mathbb{T}$ and the implicit constants in (2.11)-(2.12).

Appendix B. Proof of Proposition 3.1

In this proof, we analyze the limit $\lambda \to 0$ for a fixed $\Delta t > 0$. We denote $C_k^{(1,n+1)}$ the coefficient $C_k^{(1)}$ computed in (3.4) at time step n. Our proof is divided into 2 steps. In the first one, we solve the linearized scheme (3.4) to prove that C_0^n converges to 1, that $C^{(1,n)}$ converges to 0 and that $C_2^{(1,n)}$ remains bounded uniformly in λ. In the second step, we analyze the nonlinear scheme (3.5) and use our estimate from the first step to prove that C_1^n converges to 0 and that E^n is close to $\sqrt{2}\,T_0\,\partial_h\,C_2^n$ as $\lambda \to 0$.

The convergence of C_0^n is a consequence of the Poisson coupling between E^n and C_0^n. Indeed, taking the H^2 norm of the third line of (3.4) and replacing $C_0^{(1)}$ and $E^{(1)}$ with C_0^{n+1} and E^{n+1} thanks to the first two lines in (3.5), we deduce

$$\left\|C_0^{n+1} - 1\right\|_{h^2(\mathcal{J})} = \lambda^2\,\left\|E^{n+1}\right\|_{h^3(\mathcal{J})},$$

for all $0 \le n+1 \le T/\Delta t$. The latter relation is also valid when $n+1 = 0$. Hence, we bound the right hand side according to (3.8), which yields for all $\lambda > 0$

$$\sup_{0\le n\le T/\Delta t} \left\|C_0^n - 1\right\|_{h^2(\mathcal{J})} \le C\lambda. \tag{B.1}$$

To demonstrate that $\left(C_1^{(1,n)}\right)_{1\le n\le T/\Delta t}$ converges, we take the H^2 norm in the second line of (3.4) with $k = 0$, which yields

$$\sqrt{T_0}\left\|\,\partial_h\,C_1^{(1,n+1)}\right\|_{h^2(\mathcal{J})} = \left\|\frac{C_0^{(1,n+1)} - C_0^n}{\Delta t}\right\|_{h^2(\mathcal{J})}.$$

We take the supremum over all $1 \le n+1 \le T/\Delta t$ in the latter relation and bound the right hand side according to the first line in (B.1), which gives

$$\sup_{1\le n\le T/\Delta t}\left\|\partial_h C_1^{(1,n)}\right\|_{h^2(\mathcal{J})} \le C\lambda \quad \forall \lambda > 0, \tag{B.2}$$

where the constant $C > 0$ depends on Δt. To control the full H^3 norm of C_1, we bound the L^2 norm of C_1 with the L^2 norms of $\partial_h C_1$ thanks to a discrete Poincaré-Wirtinger inequality [5, Lemma 3.3], which reads

$$\|C_1^n\|_{l^2(\mathcal{J})} \le C\,\|\partial_h C_1^n\|_{l^2(\mathcal{J})} + C\left|\sum_{j\in\mathcal{J}} C_{1,j}^n \Delta x_j\right|.$$

We check that the total flux on the right hand side is 0 thanks to assumption (3.7) and standard computation, that is

$$\sum_{j\in\mathcal{J}} \mathcal{C}_{1,j}^{n}\,\Delta x_j \;=\; \sum_{j\in\mathcal{J}} \mathcal{C}_{1,j}^{(1,n+1)}\,\Delta x_j \;=\; 0\,,$$

for all $n \geq 0$. Therefore, we obtain

$$\|C_1^n\|_{l^2(\mathcal{J})} \;\leq\; C\,\|\partial_h C_1^n\|_{l^2(\mathcal{J})}\,, \quad \text{and} \quad \left\|C_1^{(1,n+1)}\right\|_{l^2(\mathcal{J})} \;\leq\; C\left\|\partial_h C_1^{(1,n+1)}\right\|_{l^2(\mathcal{J})}. \tag{B.3}$$

Together with (B.2), the last inequality yields

$$\sup_{1\leq n\leq T/\Delta t}\left\|C_1^{(1,n)}\right\|_{h^3(\mathcal{J})} \;\leq\; C\lambda\,, \quad \forall\lambda>0\,. \tag{B.4}$$

Next, we show that $C_2^{(1,n)}$ is bounded for all $1 \leq n \leq T/\Delta t$. To do so, we take the discrete derivative ∂_h^r, where $0 \leq r \leq 2$, of the second line of (3.4), multiply it by $\partial_h^r C_k^{(1,n+1)}$ and sum over all $k \in \{2, \ldots, N_H\}$. After a discrete integration by part with respect to $j \in \mathcal{J}$, this yields

$$\sum_{k=2}^{N_H}\left\|\partial_h^r C_k^{(1,n+1)}\right\|_{l^2(\mathcal{J})}^2 \;\leq\; \Delta t\,\sqrt{2\,T_0}\left\|\partial_h^{r+1} C_1^{(1,n+1)}\right\|_{l^2(\mathcal{J})}\left\|\partial_h^r C_2^{(1,n+1)}\right\|_{l^2(\mathcal{J})} \;+\; \sum_{k=2}^{N_H}\|\partial_h^r C_k^n\|_{l^2(\mathcal{J})}^2\,.$$

We bound $C_1^{(1,n+1)}$ on the right hand side according to (B.4) and we estimate the sum thanks to assumption (3.9). This yields

$$\left\|\partial_h^r C_2^{(1,n+1)}\right\|_{l^2(\mathcal{J})}^2 \leq C\left(\left\|\partial_h^r C_2^{(1,n+1)}\right\|_{l^2(\mathcal{J})} + 1\right).$$

Hence, we deduce that for all $\lambda > 0$, it holds

$$\sup_{1\leq n\leq T/\Delta t}\left\|\,C_2^{(1,n)}\right\|_{h^2(\mathcal{J})} \;\leq\; C\,. \tag{B.5}$$

The last step consists in proving that C_1^n is of order λ for all $1 \leq n \leq T/\Delta t$ and that E^n is close to $\sqrt{2}\,T_0\,\partial_h\,C_2^n$ for all $2 \leq n \leq T/\Delta t$ as $\lambda \to 0$. We proceed in three steps:

- we first prove that E^n is uniformly bounded in λ for all $1 \leq n \leq T/\Delta t$;
- we deduce that C_1^n is of order λ for all $1 \leq n \leq T/\Delta t$;
- we obtain that E^n is close to $\sqrt{2}\,T_0\,\partial_h\,C_2^n$ for all $2 \leq n \leq T/\Delta t$ as $\lambda \to 0$.

Let us first prove that E^n is uniformly bounded in λ for all $n \geq 1$. We take the H^1 norm in the first line of (3.4), which yields

$$\left\|E^{(1,n+1)}\right\|_{h^1(\mathcal{J})} \;\leq\; \sqrt{2}\,T_0\left\|\partial_h\,C_2^{(1,n+1)}\right\|_{h^1(\mathcal{J})} + \frac{\sqrt{T_0}}{\Delta t}\left(\left\|C_1^{(1,n+1)}\right\|_{h^1(\mathcal{J})} + \|C_1^n\|_{h^1(\mathcal{J})}\right) + T_0\left\|\partial_h C_0^{(1,n+1)}\right\|_{h^1(\mathcal{J})}.$$

On the right hand side, we estimate C_0 according to (B.1), $C_1^{(1,n+1)}$ according to (B.4), $C_2^{(1,n+1)}$ according to (B.5) and assumption (3.8) to estimate C_1^n. We obtain that for all $\lambda > 0$, it holds

$$\sup_{1\leq n\leq T/\Delta t}\|E^n\|_{h^1(\mathcal{J})} \;\leq\; C\,. \tag{B.6}$$

Next, we deduce that C_1^n is of order λ for all $1 \leq n \leq T/\Delta t$. To do so, we take the L^2 norm of the derivative of (3.5) with $k = 1$, which yields

$$\|\partial_h C_1^{n+1}\|_{l^2(\mathcal{J})} \;\leq\; \left\|\partial_h C_1^{(1,n+1)}\right\|_{l^2(\mathcal{J})} \;+\; \frac{\Delta t}{\sqrt{T_0}}\,\left\|\partial_h\left(E^{n+1}\left(C_0^{n+1}\,-\,1\right)\right)\right\|_{l^2(\mathcal{J})}\,.$$

We estimate $C_1^{(1,n+1)}$ thanks to (B.4), which gives

$$\|\partial_h C_1^{n+1}\|_{l^2(\mathcal{J})} \;\leq\; C\left(\left\|\partial_h\left(E^{n+1}\left(C_0^{n+1}\,-\,1\right)\right)\right\|_{l^2(\mathcal{J})} + \lambda\right).$$

We estimate the derivative of the product between E^{n+1} and $C_0^{n+1} - 1$, as follows

$$\|\partial_h C_1^{n+1}\|_{l^2(\mathcal{J})} \;\leq\; C\left(\|E^{n+1}\|_{l^\infty(\mathcal{J})}\,\|C_0^{n+1}-1\|_{h^1(\mathcal{J})} + \|E^{n+1}\|_{h^1(\mathcal{J})}\,\|C_0^{n+1}-1\|_{l^\infty(\mathcal{J})} + \lambda\right).$$

To estimate the L^∞ norms, we use the following Sobolev inequality, which holds true in dimension 1 and under assumption (3.10)

$$\|E^{n+1}\|_{l^\infty(\mathcal{J})} \leq C\,\|E^{n+1}\|_{h^1(\mathcal{J})}\,. \tag{B.7}$$

We deduce

$$\|\partial_h C_1^{n+1}\|_{l^2(\mathcal{J})} \leq C\left(\|E^{n+1}\|_{h^1(\mathcal{J})}\,\|C_0^{n+1}-1\|_{h^1(\mathcal{J})}+\lambda\right).$$

We estimate the norm of E^{n+1} thanks to (B.6), the norm of $C_0^{n+1}-1$ thanks to (B.1) and take the supremum over all $1 \leq n+1 \leq T/\Delta t$, we find

$$\sup_{1\leq n\leq T/\Delta t} \|\partial_h C_1^n\|_{l^2(\mathcal{J})} \leq C\lambda\,, \quad \forall \lambda > 0\,.$$

To control the full H^1 norm of C_1^n, we apply the discrete Poincaré inequality (B.3), which yields the first estimate in (3.11)

$$\sup_{1\leq n\leq T/\Delta t} \|C_1^n\|_{h^1(\mathcal{J})} \leq C\lambda\,, \quad \forall \lambda > 0\,. \tag{B.8}$$

To conclude, we prove that E^n is close to $\sqrt{2}\,T_0\,\partial_h\, C_2^n$ for all $2 \leq n \leq T/\Delta t$ as $\lambda \to 0$. To do so, we take the L^2 norm in the first line of (3.4), which yields

$$\left\|E^{(1,n+1)}-\sqrt{2}\,T_0\,\partial_h C_2^{(1,n+1)}\right\|_{l^2(\mathcal{J})} \leq \frac{\sqrt{T_0}}{\Delta t}\left(\left\|C_1^{(1,n+1)}\right\|_{l^2(\mathcal{J})}+\|C_1^n\|_{l^2(\mathcal{J})}\right)+T_0\left\|\partial_h C_0^{(1,n+1)}\right\|_{l^2(\mathcal{J})}.$$

On the right hand side, we estimate C_0 according to (B.1), $C_1^{(1,n+1)}$ according to (B.4), and C_1^n according to the latter estimate in (B.8), which yields

$$\left\|E^{n+1}-\sqrt{2}\,T_0\,\partial_h C_2^{(1,n+1)}\right\|_{l^2(\mathcal{J})} \leq C\lambda\,, \tag{B.9}$$

for all $n \geq 1$. Then, we prove that $\partial_h C_2^{(1,n+1)}$ is close to $\partial_h C_2^{n+1}$ taking the L^2 norm in (3.5) with $k=2$, which yields

$$\left\|\partial_h\left(C_2^{n+1}-C_2^{(1,n+1)}\right)\right\|_{l^2(\mathcal{J})} \leq C\left\|\partial_h\left(E^{n+1}C_1^{n+1}\right)\right\|_{l^2(\mathcal{J})}$$

We estimate the derivative of the product $\partial_h\left(E^{n+1}C_1^{n+1}\right)$ as follows

$$\left\|\partial_h\left(C_2^{n+1}-C_2^{(1,n+1)}\right)\right\|_{l^2(\mathcal{J})} \leq C\left(\|E^{n+1}\|_{l^\infty(\mathcal{J})}\,\|\partial_h C_1^{n+1}\|_{l^2(\mathcal{J})}+\|\partial_h E^{n+1}\|_{l^2(\mathcal{J})}\,\|C_1^{n+1}\|_{l^\infty(\mathcal{J})}\right).$$

Then, we apply the Sobolev inequality (B.7) to estimate the L^∞ norms in the last inequality and deduce

$$\left\|\partial_h\left(C_2^{n+1}-C_2^{(1,n+1)}\right)\right\|_{l^2(\mathcal{J})} \leq C\,\|E^{n+1}\|_{h^1(\mathcal{J})}\,\|C_1^{n+1}\|_{h^1(\mathcal{J})}\,.$$

We estimate the norm of E^{n+1} thanks to (B.6) and the norm of C_1^{n+1} thanks to (B.8), which yields

$$\left\|\partial_h\left(C_2^{n+1}-C_2^{(1,n+1)}\right)\right\|_{l^2(\mathcal{J})} \leq C\lambda\,,$$

for all $n \geq 1$. Plugging the latter estimate in (B.9) and taking the supremum over all $1 \leq n \leq T/\Delta t - 1$, we deduce the result the second estimate in (3.11)

$$\sup_{2\leq n\leq T/\Delta t}\left\|E^n-\sqrt{2}\,T_0\,\partial_h\,C_2^n\right\|_{l^2(\mathcal{J})} \leq C\lambda\,, \quad \forall \lambda > 0\,,$$

which concludes the proof.

Appendix C. Proof of Proposition 3.3

Using (3.4) and (3.5), the equations for C_0^{n+1}, C_1^{n+1} and E^{n+1} can be re-written

$$\begin{cases} \dfrac{C_0^{n+1}-C_0^n}{\Delta t} + \sqrt{T_0}\,\partial_h\left(C_1^{n+1}-\Delta t\,\dfrac{1}{\sqrt{T_0}}\,E^{n+1}\left(C_0^{n+1}-1\right)\right) = 0\,,\\[2mm] \dfrac{C_1^{n+1}-C_1^n}{\Delta t} + \sqrt{T_0}\,\partial_h\,C_0^{n+1} + \sqrt{2\,T_0}\,\partial_h\,C_2^{(1,n+1)} - \dfrac{1}{\sqrt{T_0}}\,E^{n+1}\,C_0^{n+1} = 0\,,\\[2mm] \lambda^2\partial_h E^{n+1} = C_0^{n+1}-1\,, \end{cases} \tag{C.1}$$

where $C_2^{(1,n+1)}$ corresponds to $C_2^{(1)}$ calculated during the Step 1 of the calculus of $(C_k^{n+1})_{k,\geq 0}$ knowing $(C_k^n)_{k\geq 0}$.

Then, inserting the first equation of (C.1) into the third one, we get

$$\lambda^2\,\frac{\partial_h E^{n+1} - 2\,\partial_h E^n + \partial_h E^{n-1}}{\Delta t^2} = \frac{C_0^{n+1} - 2\,C_0^n + C_0^{n-1}}{\Delta t^2}$$

$$= -\sqrt{T_0}\,\frac{\partial_h\,C_1^{n+1} - \partial_h\,C_1^n}{\Delta t} + \partial_h\left(E^{n+1}\,(C_0^{n+1}-1) - E^n\,(C_0^n - 1)\right).$$

Now, using the second and third equations of (C.1) yields

$$\lambda^2\,\frac{\partial_h E^{n+1} - 2\,\partial_h E^n + \partial_h E^{n-1}}{\Delta t^2}$$

$$= \partial_h^2\Big(\sqrt{2}\,T_0\,C_2^{(1,n+1)} + T_0\,C_0^{n+1}\Big) - \partial_h\left(E^{n+1}\,C_0^{n+1}\right) + \lambda^2\,\partial_h\left(E^{n+1}\,\partial_h E^{n+1} - E^n\,\partial_h E^n\right).$$

References

[1] K. R. Arun, N. Crouseilles, and S. Samantaray. High order asymptotic preserving and classical semi-implicit RK schemes for the Euler-Poisson system in the quasineutral limit. *J. Sci. Comput.*, 100(1):Paper No. 24, 34, 2024.

[2] C. Bardos. About a variant of the $1d$ Vlasov equation, dubbed "Vlasov-Dirac-Benney equation". In *Séminaire Laurent Schwartz-Équations aux dérivées partielles et applications.* École Polytech., Palaiseau, 2012-2013.

[3] R. Belaouar, N. Crouseilles, P. Degond, and E. Sonnendrücker. An asymptotically stable semi-Lagrangian scheme in the quasi-neutral limit. *J. Sci. Comput.*, 41(3):341–365, 2009.

[4] A. Blaustein. Structure preserving solver for Multi-dimensional Vlasov-Poisson type equations. working paper or preprint, Feb. 2024.

[5] A. Blaustein and F. Filbet. On a discrete framework of hypocoercivity for kinetic equations. *Math. Comp.*, 93(345):163–202, 2024.

[6] A. Blaustein and F. Filbet. A structure and asymptotic preserving scheme for the Vlasov-Poisson-Fokker-Planck model. *J. Comput. Phys.*, 498:Paper No. 112693, 25, 2024.

[7] A. Bobylev and I. Potapenko. On solutions of Vlasov-Poisson-Landau equations for slowly varying in space initial data. *Kinet. Relat. Models*, 16(1):20–40, 2023.

[8] A. V. Bobylev and I. F. Potapenko. Long wave asymptotics for the Vlasov-Poisson-Landau kinetic equation. *J. Stat. Phys.*, 175(1):1–18, 2019.

[9] S. Boscarino, F. Filbet, and G. Russo. High order semi-implicit schemes for time dependent partial differential equations. *Journal of Scientific Computing*, 68:975–1001, 2016.

[10] Y. Brenier. Convergence of the Vlasov-Poisson system to the incompressible Euler equations. *Comm. Partial Differential Equations*, 25(3-4):737–754, 2000.

[11] R. Caflisch, C. Wang, G. Dimarco, B. Cohen, and A. Dimits. A hybrid method for accelerated simulation of Coulomb collisions in a plasma. *Multiscale Model. Simul.*, 7(2):865–887, 2008.

[12] F. F. Chen. *Introduction to plasma physics and controlled fusion*, volume 1. Springer, 1984.

[13] P. Crispel, P. Degond, and M.-H. Vignal. An asymptotic preserving scheme for the two-fluid Euler-Poisson model in the quasineutral limit. *J. Comput. Phys.*, 223(1):208–234, 2007.

[14] N. Crouseilles, G. Dimarco, and M.-H. Vignal. Multiscale schemes for the BGK-Vlasov-Poisson system in the quasi-neutral and fluid limits. Stability analysis and first order schemes. *Multiscale Model. Simul.*, 14(1):65–95, 2016.

[15] P. Degond. Asymptotic-preserving schemes for fluid models of plasmas. In *Numerical models for fusion*, volume 39/40 of *Panor. Synthèses*, pages 1–90. Soc. Math. France, Paris, 2013.

[16] P. Degond and F. Deluzet. Asymptotic-preserving methods and multiscale models for plasma physics. *J. Comput. Phys.*, 336:429–457, 2017.

[17] P. Degond, F. Deluzet, and D. Doyen. Asymptotic-preserving particle-in-cell methods for the Vlasov-Maxwell system in the quasi-neutral limit. *J. Comput. Phys.*, 330:467–492, 2017.

[18] P. Degond, F. Deluzet, L. Navoret, A.-B. Sun, and M.-H. Vignal. Asymptotic-preserving particle-in-cell method for the Vlasov-Poisson system near quasineutrality. *J. Comput. Phys.*, 229(16):5630–5652, 2010.

[19] P. Degond, J.-G. Liu, and M.-H. Vignal. Analysis of an asymptotic preserving scheme for the Euler–Poisson system in the quasineutral limit. *SIAM Journal on Numerical Analysis*, 46(3):1298–1322, 2008.

[20] G. Dimarco, L. Mieussens, and V. Rispoli. An asymptotic preserving automatic domain decomposition method for the Vlasov-Poisson-BGK system with applications to plasmas. *J. Comput. Phys.*, 274:122–139, 2014.

[21] F. Filbet and S. Jin. A class of asymptotic-preserving schemes for kinetic equations and related problems with stiff sources. *J. Comput. Phys.*, 229(20):7625–7648, 2010.

[22] F. Filbet and T. Rey. A hierarchy of hybrid numerical methods for multiscale kinetic equations. *SIAM J. Sci. Comput.*, 37(3):A1218–A1247, 2015.

[23] F. Filbet and E. Sonnendrücker. Comparison of Eulerian Vlasov solvers. *Comput. Phys. Comm.*, 150(3):247–266, 2003.

[24] F. Filbet and T. Xiong. A hybrid discontinuous Galerkin scheme for multi-scale kinetic equations. *J. Comput. Phys.*, 372:841–863, 2018.

[25] D. Gérard-Varet, D. Han-Kwan, and F. Rousset. Quasineutral limit of the Euler-Poisson system for ions in a domain with boundaries II. *J. Éc. polytech. Math.*, 1:343–386, 2014.

[26] R. Glowinski and O. Pironneau. Finite element methods for Navier-Stokes equations. *Annual review of fluid mechanics*, 24(1):167–204, 1992.

[27] E. Grenier. Oscillations in quasineutral plasmas. *Comm. Partial Differential Equations*, 21(3-4):363–394, 1996.

[28] D. Han-Kwan and M. Hauray. Stability issues in the quasineutral limit of the one-dimensional Vlasov-Poisson equation. *Comm. Math. Phys.*, 334(2):1101–1152, 2015.

[29] S. Jin. Efficient asymptotic-preserving (AP) schemes for some multiscale kinetic equations. *SIAM J. Sci. Comput.*, 21(2):441–454, 1999.

[30] S. Jin. Asymptotic-preserving schemes for multiscale physical problems. *Acta Numer.*, 31:415–489, 2022.

[31] L. Pareschi and G. Russo. Implicit–explicit Runge–Kutta schemes and applications to hyperbolic systems with relaxation. *Journal of Scientific computing*, 25:129–155, 2005.